TTMP vol 1(1), 2024
doi: 10.30511/TTMP.2024.709795

Transactions in Theoretical and Mathematical Physics

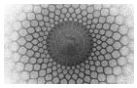

An effective technique for solving generalized Cahn-Hilliard (C-H) problems

A. Hassana[a,1], A. A. M. Arafa[b,2,3], S. Z. Rida[c,4], M. A. Dagher[d,1,5], H. M. El Sherbiny[e,6]

[1]Department of Science and Mathematical Engineering, Faculty of Petroleum and Mining Engineering, Suez University, P. O. Box: 43221, Suez, Egypt
[2]Department of Mathematics, College of Science and Arts, Qassim University, Al Mithnab, Saudi Arabia
[3]Department of Mathematics, Faculty of Science, Port Said University, Port Said, Egypt
[4]Department of Mathematics, Faculty of Science, South Valley University, Qena, Egypt
[5]Faculty of Engineering, King Salman International University, El-Tor, Egypt
[6]Department of Mathematics and Computer Science, Faculty of Science, Suez University, P. O. Box: 43221, Suez, Egypt

Received: 12 August 2023/ Accepted: 04 November 2023/ Published: 05 February 2024

Abstract Throughout this paper, we apply the Optimal Homotopy Asymptotic Method (OHAM) to find out the numerical solutions of the fractional Cahn-Hilliard (C-H) equation. We examine fractional order time-dependent partial differential equations to assess the method's competency. In the Caputo sense, fractional-order derivatives have been applied with numerical values in the closed interval [0, 1]. The biggest advantage of this method is that it contains parameters that strongly control the solution series convergence. Additionally, this method greatly simplifies calculations because it does not require any linearization, discretization, or little perturbations. Approximate solutions of the C-H equation were compared with the exact solutions; moreover, the results of the suggested method have been compared with those of other widely used numerical techniques, such as the Adomian decomposition analysis method. A comparison of these solutions with the exact solution shows that our method is more effective and accurate for solving nonlinear differential equations. MATLAB R2021b is utilized to generate the numerical results.

Keywords: Cahn–Hilliard equation, Fractional calculus, Optimal Homotopy Asymptotic Method, Numerical solutions

1 Introduction

According to the historical standpoint, fractional calculus has always been a classical calculus. Even so, in the present era, fractional calculus has wide-ranging solicitations in many technological fields, and as a result, it has more attentiveness [1,2]. Since analytical frameworks are often hard to find, very few researchers have examined their mathematical approximation approaches using the effective application of fractional systems in these disciplines. Fractional-order differential equations are useful for modelling a wide range of real-world issues. Numerous fields, including biological sciences, electromagnetic theory, electric grids, diffuse transport, groundwater problems and fluid mechanics, can benefit from the usage of these equations [3-11]. Finding the approximation of a nonlinear problem's solution is an alternative to trying to discover the exact solution, which is extremely challenging to achieve. To solve linear and nonlinear problems of FDEs, several numerical methods are used [12-22], like the Adomian Decomposition Method (ADM), Variational Iteration Method (VIM), homotopy perturbation method (HPM), and others. The previously mentioned techniques work for simple nonlinear while others work even for complex nonlinear problems. In 2008, to solve a nonlinear problem, Marinca and Herisanu [23] presented a numerical method called OHAM. The OHAM is valid not only for solving small parameters but also for nonlinear problems in science and engineering [23-27]. This strategy was then used to develop a number of solutions to large nonlinear problems across several researchers. It was shown in several of these studies that this approach is a reliable, simple, and effective tool for providing accurate analytical approximations to numerous severely nonlinear problems

[a] a.kamal@suezuni.edu.eg
[b] a.arafa@qu.edu.sa
[c] szagloul@yahoo.com
[d] mohamed.dagher@ksiu.edu.eg ; m.dagher@suezuni.edu.eg
[e] h_elsherbiny@hotmail.com

[28, 29]. Additionally, it was discovered that its essential advantage is that it's able to manage the convergence of approximate series solutions in a perfect manner. The OHAM needs only two or three terms to get an accurate solution thus, it guarantees a prompt convergence. In fact, it is the real power of this technique. The auxiliary constants (Convergence control parameters provide us with a reasonable way to ensure the convergence of OHAM series solution. By 1958, the classical Cahn–Hilliard equation (C-H equation) was introduced by the American scientists JW Cahn and J Hilliard [30]. In the field of mathematical physics, this model is one of the most studied models. Many physical phenomena, such as spinodal decomposition, phase separation, and phase ordering dynamics, are associated with this equation. Such mathematical physics equation characterizes the phase separation process through which the two components of the binary fluid are automatically separated [31-32]. Hence, this paper is organized according to the following: In section 2, an illustration of the fractional calculus definitions. Section 3 is devoted to the analysis of OHAM, and in section 4, we tackle the numerical of two problems of (CH) in the sense of the Caputo order operator. The conclusion is presented in Section 5.

2 Description of Fractional Calculus

Below I will discuss some important definitions and formulas of the theory of fractional derivatives and integrals that will be employed in this article [1,2]; we adopt the two commonly used definitions: the Caputo and its reverse operator Riemann-Liouville. That is due to Caputo fractional derivative permits traditional initial condition assumption and boundary conditions. In the following, we are going to provide the necessary remarks and basic definitions:

2.1 Riemann Liouville fractional integral

The Riemann–Liouville fractional integral of order $\alpha > 0$ of a function is $f: R^+ \to R$ given by [13]

$$J^{\alpha} f(x) = \frac{1}{\Gamma(\alpha)} \int_0^x (x-t)^{\alpha-1} f(t) dt, \alpha > 0, x > 0,$$

$$J^0 f(x) = f(x).$$

Hence, we have:

$$J^{\alpha} t^{\gamma} = \frac{\Gamma(\gamma+1)}{\Gamma(\alpha+\gamma+1)} t^{\alpha+\gamma}, \ \alpha > 0, \ \gamma > -1, \ t > 0.$$

2.2 Riemann–Liouville fractional derivative

Riemann–Liouville fractional derivatives of order α of a continuous function $f: R^+ \to R$ is obtained consecutively by

$$D^{\alpha} f(x) = D^m \big(J^{m-\alpha} f(x) \big),$$

$$D_*^{\alpha} f(x) = J^{m-\alpha} \big(D^m f(x) \big),$$

where $m - 1 < \alpha \leq m$, $m \in N$.

The Riemann–Liouville derivative has certain drawbacks when attempting to model real-world phenomena with fractional differential equations. Therefore, we will propose a modified fractional differential operator proposed by Caputo. Fractional-order differential equations, at least, are as stable as their integer-order counterpart [19].

2.3 The Caputo fractional derivative

The Caputo fractional integral of order α of a function $f: R^+ \to R$ is given by

$$D^{\alpha} f(x) = J^{m-\alpha} \big(D^m f(x) \big) = \frac{1}{\Gamma(m+\alpha)} \int_0^x (x-t)^{m-\alpha-1} f^m(t) dt,$$

where $m - 1 < \alpha \leq m, m \in N, x > 0$.

The following properties are some of the essential fractional derivatives and integrals for $\alpha, \beta \in R^+$[35]:

$$J^{\alpha} J^{\beta} f(x) = J^{\alpha+\beta} f(x),$$

$$J^{\alpha} J^{\beta} f(x) = J^{\beta} J^{\alpha} f(x),$$

$$J^{\alpha} t^{\gamma} = \frac{\Gamma(\gamma+1)}{\Gamma(\alpha+\gamma+1)} t^{\alpha+\gamma}, \ \alpha > 0, \gamma > -1, t > 0.$$

Lemma. If $-1 < \alpha \leq m$, $m \in N$, f(x) $\in C_{\mu}^m$, $\mu \geq -1$ it holds

$$D^{\alpha} J^{\alpha} f(x) = f(x),$$

$$J^{\alpha} D^{\alpha} f(x) = f(x) + \sum_{k=0}^{m-1} f^k(0^+) \frac{x^k}{k!}, \qquad x > 0.$$

3 The basic idea of the optimal homotopy analysis method (OHAM)

OHAM for fractional partial differential equations is presented in steps as follows:
Consider the following partial differential equation:

$$D\big(u(x,t) + g(x,t)\big) = 0 \, , x \epsilon \Gamma \ \ , t \geq 0 \, , \tag{1}$$

$$B\left(u, \frac{\delta u}{\delta t}\right) = 0, \tag{2}$$

where D denotes the operator which may be an integer or fractional order differential operator. x, t indicate an independent variable, $u(x,t)$ is an unknown function, B is a boundary operator and Γ is the boundary of the domain Ω, and $g(x,t)$ denotes known expression in Eq. (1).

Now, we can split the differential operator D into the terms of L, N differential operators so that:

$$L(u(x,t) + N(u(x,t) + g(x,t)) = 0,\ x\epsilon\Gamma\ . \quad (3)$$

Here, L denotes the simpler linear differential operator, which may be the linear and non-complicated portion of the Eq. (1) so that it would be solvable via any auxiliary analytical method, whereas N the operator denotes the differential operator which would be a non-linear and complicated portion of the Eq. (1).

We first construct the homotopy as:

$$(1-q)L(\phi(x,t;q)) = H(q)(L(\phi(x,t;q) + N(\phi(x,t;q)), \quad (4)$$

$$B\left(\phi(x,t;q), \frac{\delta\phi(x,t;q)}{\delta t}\right) = 0, \quad (5)$$

where $q \in [0,1]$ is an embedding parameter, $H(q)$ is a nonzero function for $q \neq 0$ and $H(0) = 0$, $\phi(x,t;q)$ is an unidentified function.

Clearly, when $q = 0$ and $q = 1$ it holds:

$$\phi(x,t;0) = u_0(x,t), \quad \phi(x,t;1) = u(x,t),$$

respectively. Therefore, when q increases from 0 to 1, the solution $\phi(x,t)$ varies from $u_0(x,t)$ to the solution $u(x,t)$ so it guarantees a rapid convergence to the exact solution.

The auxiliary function $H(q)$ gives us a simple way to manage and control the convergence while increasing the precision of the method's results and effectiveness.

The auxiliary function $H(q)$ is chosen in the form

$$H(q) = q\ c_1 + q^2 c_2 + q^3 c_3 + \cdots, \quad (6)$$

where $c_i\ , i = 1,2,3, \ldots$ are auxiliary convergence control parameters.

Expand $\phi(x,t;q,c)$ in Taylor's series about q, to find out approximate solutions as:

$$\phi(x,t;q,c_i) = u_0(x,t) + \sum_{k=1}^{\infty} u_k(x,t;c_i)\ q^k. \quad (7)$$

It was noted that the auxiliary convergence-control parameters were among the main causes of series (7) convergence.

When we substitute $\phi(x,t;q,c_i)$, and $H(q)$ in Eqs.(1-2) and equal coefficient of the same powers of q, then we get Zeroth-order and series problems, respectively:

$$L\big(u_0(x,t)\big) = 0\ , \qquad B\left(u_0(x,t), \frac{\partial u_0(x,t)}{\partial t}\right) = 0, \quad (8)$$

$$L\big(u_1(x,t)\big) = c_1\ N_0\big(u_0(x,t)\big), B\left(u_1(x,t), \frac{\partial u_1(x,t)}{\partial t}\right) = 0, \quad (9)$$

$$L\big(u_2(x,t)\big) = c_2\ N_0\big(u_0(x,t)\big) + c_1\ N_1\big(u_0(x,t), u_1(x,t)\big) + (1 + c_1)\ L\big(u_1(x,t)\big)\,, \quad B\left(u_2(x,t), \frac{\partial u_2(x,t)}{\partial t}\right) = 0\,. \quad (10)$$

The general governing k^{th}- order problem of the analytical solution is $u_k(x,t)$ in the form:

$$L\big(u_k(x,t)\big) - L\big(u_{k-1}(x,t)\big) = c_k\ N_0\big(u_0(x,t)\big) + \sum_{i}^{k-1} c_i\big[L\big(u_{k-i}(x,t)\big) + N_{k-i}\big(u_0(x,t), u_1(x,t), \ldots, u_{k-1}(x,t)\big)\big]\,, \quad k = 2,3, \ldots, \quad (11)$$

$$B\left(u_k(x,t), \frac{\partial u_k(x,t)}{\partial t}\right) = 0, \quad (12)$$

where $N_i\ , i > 0$ is the coefficient of q^i in the nonlinear operator.

$$N\ \big(u(x,t)\big) = N_0\big(u_0(x,t)\big) + qN_1\big(u_0(x,t), u_1(x,\ t)\big) + q^{\ 2}N_2\big(u_0(x,t), u_1(x,t), u_2(x,t)\big) + \cdots\,. \quad (13)$$

If series (4) converges at q = 1, one has:

$$\tilde{u}(x,t,c_i) = u_0(x,t) + \sum_{k=1}^{\infty} u_k\ (x,t;c_i),\ i = 1,\ldots\ . \quad (14)$$

Substituting Eq. (14) into Eq. (1), we get the residual as follows:

$$R(x,t;c_i) = L\big(\tilde{u}(x,t,c_i)\big) + N\big(\tilde{u}(x,t,c_i)\big), \quad i = 1, \ldots \quad (15)$$

As $R(x,t;c_i) = 0$ then $\tilde{u}(x,t,c_i)$ happens to be the same solution. Identifying the auxiliary convergence-control parameters c_1, c_2, c_3,… using a method of the following as Ritz, Least square, Collocation, and Galerkin's Method [33].

In the presentation below, to obtain the optimal values of auxiliary convergence-control parameters, the least square method is used as follows:

$$J(c_i) = \int_0^t \int_\Omega R^2(x,t,c_i)\,dx\,dt, \tag{16}$$

where R is the residual. The unidentified constants $c_i (i = 1,2,3,\dots,m)$ is optimally identifiable from the conditions:

$$\frac{\delta J}{\delta c_1} = \frac{\delta J}{\delta c_2} = \cdots = \frac{\delta J}{\delta c_m} = 0. \tag{17}$$

Obviously, in the case that the low order of m, the nonlinear algebraic system can be solved easily but the larger m is, the more difficult to solve.

4 Numerical simulations

Through this part, we are going to apply OHAM for two problems of the Time-Fractional Cahn-Hilliard Equation.

Example 1 Consider the following form of the time-fractional C-H equation [34]

$$D_t^\alpha u = u_x + 6\,u\,(u_x)^2 + (3u^2 - 1)\ ;\ 0 < \alpha \le 1, \tag{18}$$

with the initial condition

$$u(x,0) = \tanh\left(\frac{\sqrt{2}}{2}\,x\right). \tag{19}$$

The exact solution of Eq. (18)

$$u(x,t) = \tanh\left(\frac{\sqrt{2}}{2}\,(x+t)\right). \tag{20}$$

Following the OHAM formulation presented in Section 3, we have

$$L(\phi(x,t;q) = D_t^\alpha u,$$

$$N(\phi(x,t;q) = -(u_x + 6\,u\,(u_x)^2 + (3u^2-1)u_{xx} - u_{xxxx}),$$

with the initial condition:

$$\phi(x,0;q) = \tanh\left(\frac{\sqrt{2}}{2}\,x\right). \tag{21}$$

Collecting the same powers of q, and equating each coefficient of q to zero, we get the zeroth order problem:

$$\frac{\delta^\alpha u_0}{\delta t^\alpha} = 0. \tag{22}$$

Table 1 Auxiliary convergence-control parameters (c_1, c_2) of Example 1 for different values of α

α	c_1	c_2
0.8	-0.0211939932470	0.0900871779811
0.9	-2.2025E-20	0.0667761610830
0.9	-1.3814E-20	0.0686531670168
1	4.4134E-20	0.0706631567497

We begin with an initial approximation $u_0(x,t) = u(x,0) = \tanh\left(\frac{\sqrt{2}}{2}\,x\right)$, and using the initial approximation (19), we get the first order problem as:

$$\begin{aligned}\frac{\delta^\alpha u_1}{\delta t^\alpha} = -c_1 \Big(&\frac{1}{\sqrt{2}}\left(\operatorname{sech}\left(\frac{x}{\sqrt{2}}\right)\right)^2 \\ &- \left(\operatorname{sech}\left(\frac{x}{\sqrt{2}}\right)\right)^4 \tanh\left(\frac{x}{\sqrt{2}}\right) \\ &- \left(\operatorname{sech}\left(\frac{x}{\sqrt{2}}\right)\right)^2 \left(\tanh\left(\frac{x}{\sqrt{2}}\right)\right)^3 \\ &+ \left(\operatorname{sech}\left(\frac{x}{\sqrt{2}}\right)\right)^2 \tanh\left(\frac{x}{\sqrt{2}}\right)\Big).\end{aligned} \tag{23}$$

$$\begin{aligned}u_1 = \frac{-c_1\,t^\alpha}{\Gamma(\alpha+1)}\Big(&\frac{1}{\sqrt{2}}\left(\operatorname{sech}\left(\frac{x}{\sqrt{2}}\right)\right)^2 \\ &- \left(\operatorname{sech}\left(\frac{x}{\sqrt{2}}\right)\right)^4 \tanh\left(\frac{x}{\sqrt{2}}\right) - \left(\tanh\left(\frac{x}{\sqrt{2}}\right)\right)^3 \\ &+ \tanh\left(\frac{x}{\sqrt{2}}\right)\Big).\end{aligned} \tag{24}$$

Using the J^α operator which is the inverse operator of D^α in (23) we obtain:

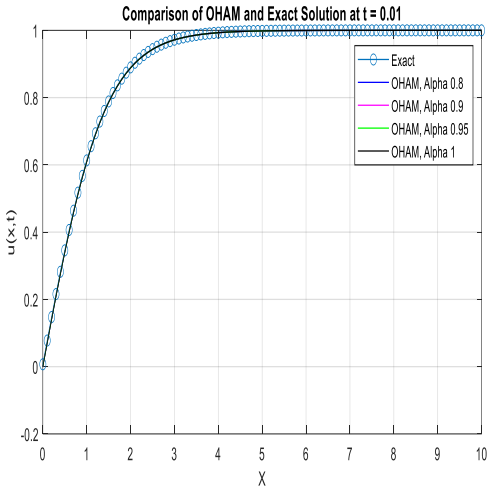

Fig.1. The numerical solutions are provided by expression (26) for Eq. (18) with different values of alpha at $t = 0.01$

By Similarity we compare the coefficient of q^2 and take J^α operator for the two sides of $\frac{\delta^\alpha u_2}{\delta t^\alpha}$ to get the value of the second-order problem:

$$u_2 = -c_1(1+c_1)\frac{t^\alpha}{\Gamma(\alpha+1)}\left(\frac{1}{\sqrt{2}}\,sech^2\left(\frac{x}{\sqrt{2}}\right) - sech^4\left(\frac{x}{\sqrt{2}}\right)\tanh\left(\frac{x}{\sqrt{2}}\right) - tanh^3\left(\frac{x}{\sqrt{2}}\right)sech^2\left(\frac{x}{\sqrt{2}}\right) + sech^2\left(\frac{x}{\sqrt{2}}\right)\tanh\left(\frac{x}{\sqrt{2}}\right)\right.$$
$$-c_2\,\frac{t^\alpha}{\Gamma(\alpha+1)}\left(\frac{1}{\sqrt{2}}\,sech^2\left(\frac{x}{\sqrt{2}}\right)\right) - 3c_2\,\frac{t^\alpha}{\Gamma(\alpha+1)}\,sech^4\left(\frac{x}{\sqrt{2}}\right)\tanh\left(\frac{x}{\sqrt{2}}\right) - (c_1)^2\,\frac{t^{2\alpha}}{\Gamma(2\alpha+1)}\,(sech^2\left(\frac{x}{\sqrt{2}}\right)\tanh\left(\frac{x}{\sqrt{2}}\right))$$
$$-\frac{12}{\sqrt{2}}\,(c_1)^2\frac{t^{2\alpha}}{\Gamma(2\alpha+1)}\,sech^4\left(\frac{x}{\sqrt{2}}\right)tanh^2\left(\frac{x}{\sqrt{2}}\right) + 3\,(c_1)^2\frac{t^{2\alpha}}{\Gamma(2\alpha+1)}\,\,sech^4\left(\frac{x}{\sqrt{2}}\right)\,(\frac{1}{\sqrt{2}}\,sech^2\left(\frac{x}{\sqrt{2}}\right)$$
$$-sech^4\left(\frac{x}{\sqrt{2}}\right)\tanh\left(\frac{x}{\sqrt{2}}\right) - tanh^3\left(\frac{x}{\sqrt{2}}\right)sech^2\left(\frac{x}{\sqrt{2}}\right) + sech^2\left(\frac{x}{\sqrt{2}}\right)\tanh\left(\frac{x}{\sqrt{2}}\right))$$
$$-\,(c_1)^2\,\frac{t^{2\alpha}}{\Gamma(2\alpha+1)}\left(52\,sech^4\left(\frac{x}{\sqrt{2}}\right)tanh^3\left(\frac{x}{\sqrt{2}}\right) - 34\,sech^6\left(\frac{x}{\sqrt{2}}\right)\tanh\left(\frac{x}{\sqrt{2}}\right)\,\,-4\,sech^2\left(\frac{x}{\sqrt{2}}\right)tanh^5\left(\frac{x}{\sqrt{2}}\right)\right)$$
$$-c_2\,\frac{t^\alpha}{\Gamma(\alpha+1)}\left(\,sech^2\left(\frac{x}{\sqrt{2}}\right)\tanh\left(\frac{x}{\sqrt{2}}\right)\right) - \,(c_1)^2\,\frac{t^{2\alpha}}{\Gamma(2\alpha+1)}\left(-2\,sech^2\left(\frac{x}{\sqrt{2}}\right)tanh^3\left(\frac{x}{\sqrt{2}}\right) + 4\,sech^4\left(\frac{x}{\sqrt{2}}\right)\tanh\left(\frac{x}{\sqrt{2}}\right)\right)$$
$$-6\,(c_1)^2\,\frac{t^{2\alpha}}{\Gamma(2\alpha+1)}\,sech^2\left(\frac{x}{\sqrt{2}}\right)tanh^2\left(\frac{x}{\sqrt{2}}\right)\left(\frac{1}{\sqrt{2}}\,sech^2\left(\frac{x}{\sqrt{2}}\right) - sech^4\left(\frac{x}{\sqrt{2}}\right)\tanh\left(\frac{x}{\sqrt{2}}\right) - tanh^3\left(\frac{x}{\sqrt{2}}\right)sech^2\left(\frac{x}{\sqrt{2}}\right.\right.$$
$$\left.\left.+sech^2\left(\frac{x}{\sqrt{2}}\right)\tanh\left(\frac{x}{\sqrt{2}}\right)\right)\right) + 3\,(c_1)^2\,\frac{t^{2\alpha}}{\Gamma(2\alpha+1)}tanh^2\left(\frac{x}{\sqrt{2}}\right)\left(-2\,tanh^3\left(\frac{x}{\sqrt{2}}\right)sech^2\left(\frac{x}{\sqrt{2}}\right) + 4\,sech^4\left(\frac{x}{\sqrt{2}}\right)\tanh\left(\frac{x}{\sqrt{2}}\right)\right)$$
$$+3\,c_2\,\frac{t^\alpha}{\Gamma(\alpha+1)}\,tanh^3\left(\frac{x}{\sqrt{2}}\right)sech^2\left(\frac{x}{\sqrt{2}}\right) \qquad (25)$$

By using the initial condition (19), Eq. (24), and Eq. (25), we find out second-order approximate solution of Eq. (18)

$$u(x,t) = \,u_0(x,t) + \,u_1(x,t) + \,u_2(x,t) + \cdots \qquad (26)$$

Through the least squares method mentioned in Section 3, we obtain the values of constants c_1, c_2 for different values of α. See Table 1.

Example 2 We will tackle the nonlocal fractional order (C-H equation) with terms of advection and reaction [35], which is defined as

$$D_t{}^\alpha u - 6\,u\,(u_x)^2 - (3u^2-1)u_{xx} \,\, + u_{xxxx} - \beta\,u_x - k(u-u^2) = 0, \qquad (27)$$

where k reaction term and β advection term. With the initial condition

$$u(x,0) = x. \qquad (28)$$

Without exact solutions we will apply the OHAM steps.

Table 2 The results of the second order solution (26) of OHAM method at different values α

t	x	Exact	OHAM α = 0.8	OHAM α = 0.9	OHAM α= 0.95	OHAM α = 1	Error OHAM α = 1	Error ADM α = 1
0.002	0.1	0.072	0.07034	0.07041	0.07045	0.07049	0.00150	0.00281
0.002	0.2	0.1418	0.14024	0.14031	0.14035	0.14039	0.00148	0.00278
0.002	0.3	0.2103	0.20876	0.20883	0.20888	0.20891	0.00144	0.002709
0.004	0.1	0.0734	0.07015	0.07025	0.07033	0.07039	0.00301	0.005645
0.004	0.2	0.14326	0.14005	0.14015	0.14023	0.14029	0.002967	0.0055630
0.004	0.3	0.21171	0.20858	0.20868	0.20876	0.20882	0.002894	0.0054236
0.006	0.1	0.07481	0.069986	0.070104	0.070211	0.070295	0.004518	0.0084799
0.006	0.2	0.14464	0.13989	0.14000	0.14011	0.14019	0.004450	0.0083498
0.006	0.3	0.21306	0.20842	0.20854	0.20864	0.20872	0.004340	0.0081448
0.01	0.1	0.07762	0.06968	0.069819	0.069972	0.070096	0.007529	0.0141747
0.01	0.2	0.14741	0.13959	0.13972	0.13987	0.14	0.007414	0.0139581
0.01	0.3	0.21576	0.20813	0.20826	0.20841	0.20853	0.00722	0.013609

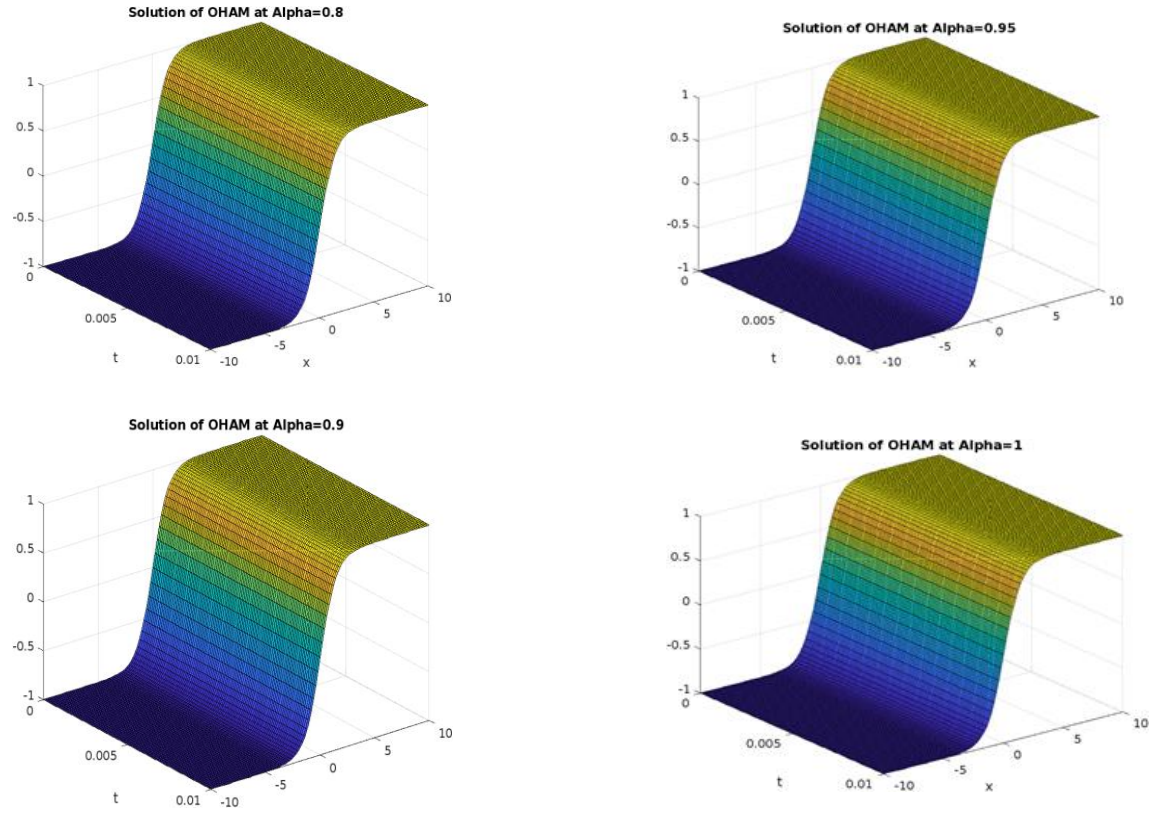

Fig.2. The numerical solutions are presented by expression (26) for Eq.18 with different values of Alpha at $t = 0.01$.

We are considering differential operators for Eq. (27) as:

$$L(\phi(x,t;q) = D_t^{\alpha} u,$$

$$N(\phi(x,t;q) = -6\,u\,(u_x)^2 - (3u^2-1)u_{xx} + u_{xxxx} - \beta\,u_x - k(u - u^2).$$

With the initial condition:

$$\phi(x,0;q) = x. \tag{29}$$

The zeroth order problem is the first one of these and it is written as follows:

$$\frac{\delta^{\alpha} u_0}{\delta t^{\alpha}} = 0. \tag{30}$$

We begin with an initial approximation $u_0(x,t) = u(x,0) = x$, we get the first order problem is:

$$\frac{\delta^{\alpha} u_1}{\delta t^{\alpha}} = -c_1\,(\,6x + \beta + \mathrm{k}\,x - \mathrm{k}x^2\,). \tag{31}$$

By using the J^{α} operator for the two sides of (31) we get:

$$u_1 = \frac{-\,c_1\,t^{\alpha}}{\Gamma(\alpha+1)}\,(\,6x + \beta + \mathrm{k}\,x - \mathrm{k}x^2\,). \tag{32}$$

By Similarity we compare the coefficient of q^2 and take J^{α} operator for the two sides of $\frac{\delta^{\alpha} u_2}{\delta t^{\alpha}}$ to get the value of the second-order problem:

$$u_2 = \frac{t^{\alpha}}{\Gamma(\alpha+1)}\,(\,-c_1(1+c_1) + 6x + \beta + \mathrm{k}\,x - \mathrm{k}x^2 - \beta c_2 - 6c_2\,x - kc_2\,x + kc_2\,x^2\,) + {c_1}^2\frac{t^{2\alpha}}{\Gamma(2\alpha+1)}(\,(2k) + 12\beta + 2\mathrm{k}\,\beta + (2k)x^3 + x^2(-48k - -3k^2) + x(108 + 24k + k^2 - 4\mathrm{k}\,\beta). \tag{33}$$

By using the initial condition (27), Eq. (32), and Eq. (33), we find out second-order approximate solution of Eq. (27)

$$u(x,t) = u_0(x,t) + u_1(x,t) + u_2(x,t) + \cdots, \tag{34}$$

while through using the least squares method mentioned in Section 3, we obtain the values of constants c_1, c_2 for different values of k and α. Check Tables 3-5.

Table 3 Auxiliary convergence-control parameters (c_1, c_2) of Example 2 for different value of α at $\beta = -1, x = 1$

α	k	c_1	c_2
0.8		-8.0452e-15	0.16381
0.9	1	2.9374e-15	0.17061
1		1.7577e-15	0.17854

Table 4 Auxiliary convergence-control parameters (c_1, c_2) of Example 2 for different values of α at $\beta = -1, x = 1$

α	k	c_1	c_2
0.8		-1.8637e-14	0.20398
0.9	-1	-5.2333e-15	0.21185
1		3.4992e-16	0.22094

Table 5 Auxiliary convergence-control parameters (c_1, c_2) of Example 2 for different values of α at $\beta = -1, x = 1$

α	k	c_1	c_2
0.8		2.9374e-15	0.21274
0.9	0	-5.7462e-14	0.22459
1		6.4766e-15	0.2363

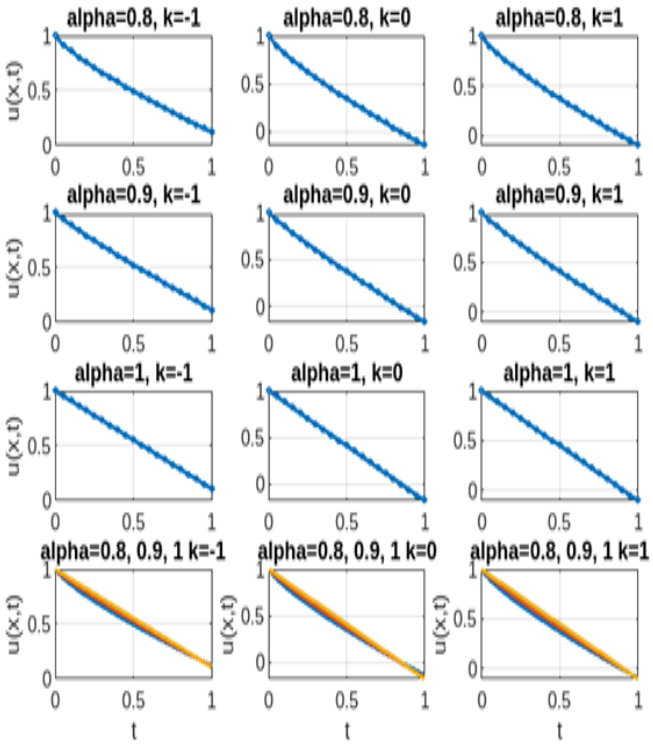

Fig.3. The numerical solutions are shown in expression (34) for Eq. (27) in different values of alpha and various values of k, $\beta = -1, x = 1$.

5 Conclusion

In this study, we implement OHAM to accurately solve the C-H equations. The accuracy of these results has been shown in Tables 1-5 and they have been shown graphically in Figures 1-3 in order to highlight the efficiency and distinction of this method. The technique convergence is regulated by a flexible function known as the auxiliary function. The Caputo derivative fractional-order and the well-known least squares technique are used to determine the values of the unknown arbitrary constants in the auxiliary function. In the Caputo meaning, fractional-order derivatives are taken with results in the closed interval [0, 1]. The proposed technique is immediately applicable to Cahn-Hilliard equations, and no small or large parameter assumptions are required. Also, studies on this topic may lead to more interesting conclusions and results. Thus, it offers more realistic solutions to real physical problems.

References

1. R. Gorenflo and F. Mainardi, *Fractional calculus, in Fractals and fractional calculus in continuum mechanics. International Centre for Mechanical Sciences* (Springer, Vienna, 1997)
2. I. Podlubny, *Fractional differential equations* (Academic Press, New York, 1999)
3. I. Podlubny, *Fractional Differential Equations: An Introduction to Fractional Derivatives, Fractional Differential Equations, to Methods of Their Solution and Some of Their Applications* (Elsevier, 1998)
4. L. Debnath, Journal of Mathematics and Math. Sc. **2003**, 54 (2003)
5. K. S. Miller and B. Ross, *an Introduction to the Fractional Calculus and Fractional Differential Equations* (Wiley, 1993)
6. K. F. Nishimoto, *Calculus, Integrations and Differentiations of Arbitrary Order* (Descartes Press, 1984)
7. A. Ali et al., Alexandria Engineering J. **61**, 6 (2022)
8. X. H. Zhang, A. Ali, M. A. Khan, M. Y. Alshahrani, T. Muhammad, S. Islam, Discrete Dyn. in Nature and Society **2021** (2021)
9. A. Ali, F. S. Alshammari, S. Islam, M. A. Khan, S. Ullah, Results in Phys. **20** (2021)
10. M. A. Aba Oud, A. Ali, H. Alrabaiah, S. Ullah, M. A. Khan, S. Islam, Advances in Difference Eq. **2021**, 1 (2021)
11. A. Rehman, Z. Salleh, T. Gul, Journal of Advanced Research in Fluid Mechanics and Thermal Sc. **81**, 2 (2021)
12. S. A. El-Wakil, A. Elhanbaly, M. A. Abdou, Appl. Math. Comput. **182** (2006)

13. V. Daftardar-Gejji, H. Jafari, J. Math. Anal. Appl. **301** (2005)
14. G. Wu, Comput. Math. Appl**. 61** (2011)
15. Sh. Yang, A. Xiao, H. Su, Comput. Math. Appl. **60** (2010)
16. P. K. Gupta, M. Singh, Comput. Math. Appl. **61** (2011)
17. O. Abdulaziz, I. Hashim, S. Momani, J. Comput. Appl. Math. **216** (2008)
18. A. A. M. Arafa, A. M. S. Hagag, Asian-Eur. J. Math. **12** (2019)
19. A. A. M. Arafa, A. M. S. Hagag, Chinese J. Phys. **60** (2019)
20. M. Khan et al., Math. Comput. Modelling **55** (2012)
21. Z. Odibat, S. Momani, Appl. Math. Lett. **21** (2008)
22. O. Abu-Arqub, J. Adv. Res. Appl. Math. **5** (2013)
23. V. Marinca, N. Herişanu, International Comm. in Heat and Mass Transfer **35** (2008)
24. K. A. Gepreel, T. A. Nofal, Math Sci **9** (2015)
25. O. O. Okundalaye, W. A. M. Othman, N. Kumaresan, **2020** (2020)
26. H. M. Younas, M. Mustahsan, T. Manzoor, N. Salamat, S. Iqbal, Mathematics **7** (2019)
27. A.K. Gupta, S. Saha Ray, Computers & Fluids **103** (2014)
28. V. Marinca, N. Herişanu, Appl. Math. Comput. **231**, (2014)
29. R. K. Pandey, O. P. Singh, V. K. Baranwal, M. P. Tripathi, Comput. Phys. Commun **183** (2012)
30. J. W. Cahn, J. Hilliard, Free energy of a nonuniform system. I. interfacial free energy, J. Chem. Phys. **28** (1958)
31. A. Berti, I. A Bochicchio, Math Method Appl Sci **34** (2011)
32. G. Akagi, G. Schimperna, A. Segatti, J Differ. Equations **261** (2016)
33. W. Alhejaili, E. S. Alhazmi, R. Nawaz, A. Ali, J. K. K. Asamoah, L. Zada, Hindawi Journal of Nanomaterials **2022** (2022)
34. Z. Dahmani1, M. Benbachir, International Journal of Nonlinear Science **8**, 1 (2009)
35. N. K. Tripathi, S. Das, S. Hong, H. Jafari, M. M. Al Qurashi, Advances in Mechanical Engineering **9**, 12 (2017)

TTMP vol 1(1), 2024
doi: 10.30511/TTMP.2023.709327

Transactions in Theoretical and Mathematical Physics

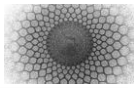

Statistical Investigation of Electron Density of Laser-Air Interaction System Using Saha Relation in Local Thermodynamic Equilibrium

A .H. Ahooee[a], E. Hajiali , N. Amiri Rad, D. Shahabi

Department of Photonics, Faculty and Research Institute of Basic Sciences, Imam Hossein Comprehensive University, Tehran, Iran

Received: 15 July 2023/ Accepted: 13 December 2023/ Published: 05 February 2024

Abstract: Investigating complex systems and accessing information has been of interest to researchers for years. The desired system in this research includes the investigation of the plasma resulting from the interaction of the laser with the desired substance of the research. Air is the material of choice for producing plasma in interaction with the laser. We used Nd:YAG laser for incident beam to interact with air matter. Plasma was formed by the interaction of laser with air. In the following, it is possible to check the plasma density by scanning the plasma resulting from the interaction of the laser with air. Therefore, in order to determine the electron density by the Saha method, we first need to calculate the electron temperature, which was calculated using the spectral line pair intensity ratio method of the plasma temperature equal to Kelvin. In the continuation of the research, the electron density was measured using Saha's equation.

keywords: Laser-plasma interactions, Plasma temperature and density, Laser spectroscopy, Saha equation

1 Introduction

Various lasers such as Nd:YAG, Excimer, co_2 and Microchip lasers are used for the formation of plasma according to the type of research, and the type of laser has been selected for the research according to the characteristics listed in table 1 [1-4].

In this research, we created Nd:YAG laser by setting up the laser and we used laser induced breakdown method (LIBS) to create plasma, in this method an short Q-switch pulse from a Nd:YAG laser with high energy density on the target surface is focalized. Focusing the laser on the sample causes a rapid increase in the surface temperature of the sample. In such a way, the material below the surface reaches critical temperature and pressure, leading to surface explosion. The material is absorbed by energy from the pulse of the laser, evaporation, atomized and ionized and thus plasma is formed. In this study, the Nd:YAG laser was focused on the air and the plasma produced by the interaction of the laser with the air was formed. Using a spectrograph, we recorded the spectral spectra of plasma resulting from laser interaction with air, and using the obtained spectrophotometer results, electron temperature was determined by the spectral line pairing method, and the electron density was calculated using the Saha relation.

2 Materials and method, calculations, governing equation

2.1 Local Thermodynamic Equilibrium

The thermodynamic equilibrium of the system is a state of the system in which none of the properties of the system changes with the passage of time. Complete thermodynamic equilibrium is achieved by establishing equilibrium in the four processes of kinetic equilibrium, excitation, ionization, and radiation. In such a plasma, electron and ion velocity distribution follows the Maxwell-Boltzmann distribution function and the distribution of excited states follows the Saha-Boltzmann type and photons follow the Planck energy distribution function [5]. When photons escape from the plasma in the radiation process, their energy distribution no longer follows the Planck distribution and inevitably affects the balance of electrons, ions and atoms. However, if the energy dissipated by plasma radiation is less than the energy involved in other processes and energy exchange, the condition of complete thermodynamic equilibrium (TE) is not possible, while the three processes of equilibrium-kinetic, excitation and ionization have equilibrium. are local thermodynamics and the Maxwell and Saha-Boltzmann distributions are still valid to describe the system. A new equilibrium is defined as local thermodynamic equilibrium (LTE). This equilibrium is local because it exists only in a small area of the plasma volume and the temperature will be different from one area to another in the plasma. Due to the large number of collisions in the plasma, the temperature will be the same in the whole plasma region with a good approximation, and the calculated temperature will be an average of the temperature in the whole plasma region [5].

Measurement of plasma parameters is possible only if the plasma is in local thermodynamic equilibrium. In this condition, it is assumed that the plasma has reached equilibrium and its parameters, such as its temperature and electron density, are constant and measurable [5].

[a] e-mail: alirezaht96@gmail.com

Table 1 Characteristics of lasers used in LIBS [4][6]

Features related to applications in LIBS	Repeat Rate (Hz)	pulse length (ns)	Wave-length (nm)	Laser type
Easy access to harmonic			Harmonic:	
Excellent beam quality		6-15	Main: 1064	
Ability to produce double tap	1-20	4-8	Second: 532	Nd:YAG
Pump by Lamp and Diod Pump			Third: 355	
			Forth: 255	
Requires periodic gas charging			XeCl: 308	Excimer
Producing UV wavelengths	200	20	KrF: 248	
			ArF: 194	
Requires periodic gas charging	200	200	10600	CO_2
Good quality of beam and fashion	1-10K	<1	1064	Microchip
Capable of producing tap to high pulse				
High repetition rate				

2.2 Method of the intensity ratio of two lines of one element

The most important factor in plasma radiation is plasma temperature and precise determination of plasma temperature is important. Plasma temperature is often used for the same element as the size of the intensity ratios of ion-to-neutral lines or neutral lines. In the first case, line intensities are combined with equation and electron density measurement to determine plasma ionization temperature.

$$\frac{I_{i+1}}{I_i} = 2 \times \frac{(2\pi m_e k_B T)^{\frac{3}{2}}}{n_e^2} \left(\frac{gA}{\lambda}\right)_{i+1} \left(\frac{gA}{\lambda}\right)_i \times \exp\left[\frac{-(IP_I + E_{i+1} + E_i)}{k_B T}\right]. \quad (1)$$

Here I is the area below the absorption line of ions and atoms, N_e is the electron density, g is the statistical weight factor, and A is the Einstein coefficient for spontaneous emission of the higher level, λ and T are the wavelength and temperature of the plasma, respectively. IP_I, E_{i+1} and E_i are the ionization potentials of the atom, the ion line excitation energy and the ionization energy of the atomic line, respectively. k_B Boltzmann constant and h is Planck constant [7]. In the second case, line intensities are combined with the Boltzmann equation to determine the temperature of the plasma excitation and the relation (2) expresses that:

$$\frac{I_1}{I_2} = \frac{g_1 A_1 \lambda_2}{g_2 A_2 \lambda_1} \exp\left(-\frac{E_1 - E_2}{k_B T}\right), \quad (2)$$

and thus, T is equal to [7, 8]:

$$T = \frac{E_1 - E_2}{k_B \ln\left[\frac{I_1 g_2 A_2}{I_2 g_1 A_1}\right]}, \quad (3)$$

where the indices 1 and 2 are related to separate lines. With an increase in energy, the difference between E_1 and E_2, accuracy in determining plasma temperature increases. This accuracy is increased by measuring the number of different pairs of lines and averaging the number of different lines. However, it is important to note that measurement accuracy is strongly dependent on factor A. Plasma temperature is one of the most important parameters in determining electron density and the concentration of plasma constituent elements [9].

2.3 Density measurement using the Saha relation

If the plasma is considered to be localized in thermodynamic equilibrium, the density of the electron can be calculated using the ratio of the intensity of different ionization states of an element, while the Saha equation is written in terms of the density ratio of the total number of two ionizing states corresponding to an element. The electron density of plasma can be calculated by considering two lines with different degrees of ionization and using the relation (4) known as the Saha equation:

$$n_e \frac{I_2}{I_1} = 2\left(\frac{2\pi m_e}{h^2}\right)^{3/2} (kT)^{3/2} \frac{U^{II}(T)}{U^{I}(T)} e^{-E_{ion}/kT} \quad . \quad (4)$$

In this regard m_e the mass of the electron, h is the Planck constant, k is Boltzmann's constant, E_{ion} ionization energy in electron Volts and T is plasma temperature in Kelvin.

$U^I(T)$ and $U^{II}(T)$ are the partition function with ionization of the first and second order at the plasma temperature and n^I and n^{II} are the number of photons emitted from the plasma in these states and n_e the electron density of plasma is obtained in terms of cm^{-3} [5].

3 Results and Discussion

Laser plasma was formed from Nd:YAG laser with air It is collected by the lens of light emitted from plasma and

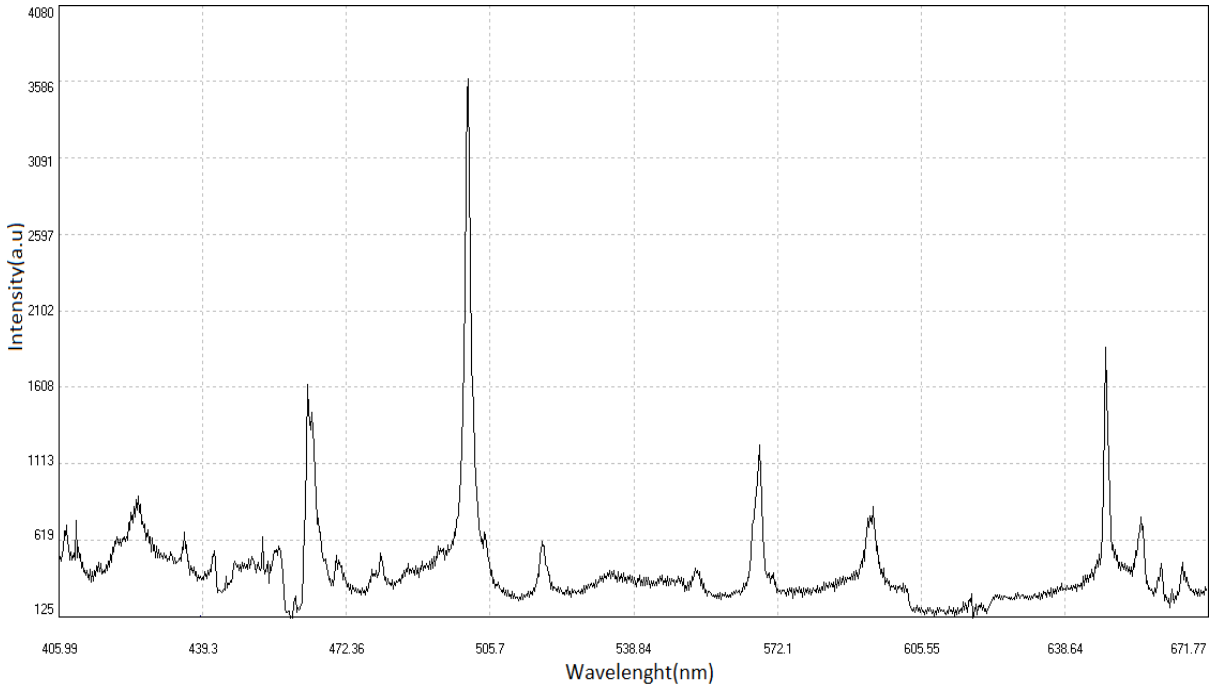

Fig.1 Spectral Spectra Plasma from Laser Interaction with Air in the range of 405.99-671.77 nm

Table 2 Nitrogen Elements Detected from Figure 1 [10]

Standard wave-length	Observed wave-length	element
409.99	409.99	NI
444.70	444.67	NII
460.71	460.62	NII
616.77	616.76	NII
648.17	648.25	NI
661.05	661.08	NII
665.65	665.63	NI

with the help of the CCD-Array Toolkit software, the plasma spectra of the air are observed in the laptop. Figure 1 shows the plasma spectra resulting from the interaction of the laser with air. In Table 2, nitrogen elements observed from the spectra of air plasma in the range of 405.99-671.77 nm are shown, and the emission lines of the spectrograph are shown in Table 3.

$$\frac{I_2}{I_1} = \frac{g_2 A_2}{g_1 A_1} \exp\left(-\frac{E_2 - E_1}{KT}\right),$$

$$\frac{741}{380} = \frac{4 \times 0.348}{5 \times 11.2} exp\left(-\frac{13.702 - 23.196}{0.86 \times 10^{-4} \times T}\right),$$

$$\rightarrow T = 2.5172 \times 10^4 K,$$

and for the rest of the two lines ratios are calculated as follows, the statistical results of which are given in Table 4.

In the following, the electron density is also calculated by the Saha-Boltzmann method:

$$n_e \frac{I_2}{I_1} = 2\left(\frac{2\pi m_e}{h^2}\right)^{3/2} (kT)^{3/2} \frac{U^{II}(T)}{U^I(T)} e^{-E_{ion}/kT},$$

$$2\left(\frac{2\pi m_e}{h^2}\right)^{3/2} = 6.5 \times 10^{21}, \quad k = 0.86 \times 10^{-4} \text{ eV}.$$

Table 3 Specification of Horizontal Emission Lines of Figure 1 [10]

Standard wavelength	I	element	$A_{ki} \times 10^7$	$E_k(eV)$	g
409.99	741	N I	0.348	13.702	4
444.70	380	N II	11.2	23.196	5
460.71	250	N II	3.15	21.152	3
616.77	226	N II	2.65	25.151	7
648.17	1863	N I	0.343	13.662	4
648.20	520	N II	2.58	20.409	3
661.05	458	N II	6.01	23.474	7
665.65	485	N I	0.217	13.614	2

Table 4 Calculation of temperature results with the ratio of two different lines

No	Line element (1) (wavelength)	Line element (2) (wavelength)	$T(K)$
1	NI (409.99)	NII (444.70)	2.5172×10^4
2	NI (409.99)	NII (460.71)	2.8859×10^4
3	NII (616.77)	NI (648.17)	2.8342×10^4
4	NI (648.17)	NII (661.05)	2.3641×10^4
5	NII (648.20)	NI (665.65)	2.8104×10^4
6	NII (661.05)	NI (665.65)	2.4756×10^4

Considering the relationship (4), we need the partition functions and ionization energy proportional to two lines; these parameters are obtained from library data and collected in Table 5.

Table 5 Data needed for Saha relations [10]

No	Scattering function of a single ionized element	Scattering function of a doubly ionized element	Ionization energy*(eV)*
1	11.38	11.63	14.5341
2	15.74	12.19	14.5341
3	15.02	12.11	14.5341
4	10.07	11.41	14.5341
5	14.69	12.07	14.5341
6	11.01	11.57	14.5341

Number (1) in table (5): For two lines N I (409.99) and N II (444.70) the Scattering function is $U^I = 11.38$ and $U^{II} = 11.63$ and its ionization energy is $E_{ion} = 14.5341$, and thus the electron density is calculated for these two lines:

$$n_e \frac{380}{741} = (6.05 \times 10^{21})(2.164)^{\frac{3}{2}} \frac{11.63}{11.38} e^{-\frac{14.5341}{2.164}},$$

$$\rightarrow n_e = 4.6619 \times 10^{19}\text{cm}^{-3}.$$

And for the rest of the lines, it is calculated as follows: the statistical results are given in Table 6.

Table 6 Results of Density Calculation with Saha Equation

No	element Once ionized (Wavelength)	element double ionized (Wavelength)	$\text{n}_\text{e}(\text{cm}^{-3})$
1	NI (409.99)	N II (444.70)	4.6619×10^{19}
2	NI (409.99)	N II (460.71)	1.5543×10^{20}
3	NI (648.17)	N II (616.77)	3.9362×10^{20}
4	NI (648.17)	N II (661.05)	6.3534×10^{19}
5	NI (665.65)	N II (648.20)	4.2609×10^{19}
6	NI (665.65)	N II (661.05)	2.2682×10^{19}

4 Conclusion

In this research, the values of temperature and electron density for plasma produced by laser interaction with air have been calculated. To determine the electron temperature, spectral line pairing method was used. Considering the results of temperature calculations from Table 4, the value 2.6479×10^4 was determined for the electron temperature and Saha equation was used to calculate the electron density and by means of the results of the calculations of electron density from table (6) the value of $2.5914 \times 10^{20}\ cm^{-3}$ for the electron density was obtained.

References

1. R. Knopp, F. J. Scherbaum, J. I. Kim, Fresenius. J. Anal. Chem. **355**, 1 (1996). doi: 10.1007/s0021663550016, and P.C. Brans, U.G. Meissner, Eur. Phys. J. C **40**, 97 (2005)
2. L. Radziemski, D. Cremers, Spectrochim. Acta Part B: At. Spect. **87** (2013). doi: 10.1016/j.sab.2013.05.013
3. S. J. J. Tsai, S. Y. Chen, Y. S. Chung, P. C. Tseng, Analytical Chemistry, **78**, 21 (2006). Doi: 10.1021/ac060749d.
4. S. N. T. Jagdish, P. Singh, *Laser-Induced Breakdown Spectroscopy* (Elsevier 2007

5. A. W. Miziolek, V. Palleschi, I. Schechter, *Laser-Induced Breakdown Spectroscopy (LIBS)* (Cambridge University Press, 2006)
6. F, Khalilinejad, *Analysis of dense liquids using Laser Induced Breakdown Spectroscopy (LIBS) by IR wavelength of Q-switch YAG Laser* (Alzahra University, 2012)
7. D. A. Cremers, L. J. Radziemski, *Handbook of Breakdown Spectroscopy* (John Wiley & Sons 2006)
8. T. P. Hughes, J. E. Bayfield, Phys. Today **30**, 4 (1977). doi: 10.1063/1.3037501
9. M. M. H. Matin, *Increasing plasma radiation by applying electrical spark on laser-induced breakdown* (beheshti university, 2019)
10. physics.nist.gov, National Institute of Standards and Technology

TTMP vol 1(1), 2024
doi: 10.30511/TTMP.2024.709741

Transactions in Theoretical and Mathematical Physics

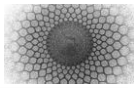

Numerical study of the spot size changes of a guided laser pulse through a plasma channel with a density profile with radial and longitudinal variation

M. Ghalandari[1,a], B. Babayar-Razlighi [2,b*]

[1] Department of Energy Engineering and Physics, Faculty of Electrical and Computer Engineering, University of Science and Technology of Mazandaran, Behshahr, Iran
[2] Department of Mathematics, Qom University of Technology, P. O. Box 1519-37195, Qom, Iran

Received: 06 May 2022/ Accepted: 15 December 2023/ Published: 05 February 2024

Abstract: In this paper, guiding of Gaussian laser pulse in plasma channel is numerically investigated. We assumed that the plasma channel has radial and longitudinal changes. We obtained the matched condition for guiding of high-intensity laser pulses through the plasma channel. Using the source-dependent expansion (SDE) method, we extracted four paired equations for pulse amplitude, phase, spot size and inverse of the radius of wave front curvature. Numerical results of equations were obtained using the Runge-Kutta numerical method. Numerical results showed that the normalized laser spot size during propagation in the plasma channel is constant in the matched mode and oscillates for the mismatched mode. The Runge-Kutta method of order 4 has good results for well posed problems. We have considered the functional form of the model and in this work we have shown that our problem is well posed, so the proposed method has satisfactory numerical results. The numerical results confirm this concept.

Keywords: Guiding, Runge-Kutta, Matched condition, Plasma channel, Spot size

1 Introduction

Propagation of high intensity lasers in plasma is closely related to wide range of applications such as x-ray lasers, high harmonics generation and wake field acceleration [1-3]. These applications have motivated researchers to study the underlying physics of the interaction between high-intensity laser and matter. In a medium, the propagation coefficients of a high-intensity laser can be significantly different from that of a vacuum. The characteristic length associated with the laser beam diffraction is in which λ corresponds to wavelength and R_{s0} is laser spot size in vacuum. Optical guiding is a method for increasing the propagation's distance in plasma. Optical guiding based on refraction change, however, is only possible when the radial index of refractive index n has a maximum on axis; that is $\partial n/\partial r<0$. When this condition is met, phase velocity $v_p=c/n$ on axis (r=0) becomes smaller than that of the off-axis. This, in turn, converges the laser's phase front in a way that the laser beam focuses toward the axis. The refractive index of the center of an inhomogeneous plasma channel will be higher than its periphery, as long as the density of electrons in center remains smaller than the periphery density. A plasma channel with such a refractive index causes optical guiding of the laser pulse. Several methods of guiding, such as relativistic guiding [4, 5], Z-pinch waveguide [6], grazing incidence waveguide [7, 8], gas-filled capillary discharge [9, 10] have been successfully examined. In this paper, the optical guiding of a laser pulse inside a plasma channel, along with the variation of radius and longitude of the laser, will be discussed.

The organization of this paper is as follows. The equations for the laser wave envelope and matched conditions are derived in Sec. 2. In Sec. 3, numerical results of the guided laser pulse propagating through the plasma channels are presented. In Sec. 4, we show that the equations (12-15) define a well-posed problem, and the Runge-Kutta method of order 4 is applicable to them. Finally, in Section 5, the results and discussions are given.

2 Guiding a high-intensity Gaussian laser pulse through the plasma channel

Laser electric field formula obtained from Maxwell equations is defined as follows:

* Corresponding author
[a] e-mail: ghalandari@qut.ac.ir
[b] e-mail: babayar@qut.ac.ir & bbabayar@gmail.com

$$(\nabla_{\perp}^2 + \frac{\partial^2}{\partial z^2} - \frac{1}{c^2}\frac{\partial^2}{\partial t^2})\vec{E}(\vec{r},t) = \vec{S}(\vec{r},t), \quad (1)$$

in which $s(\vec{r},t)$ represents the source term. Electric field $E(\vec{r},t)$ and $s(\vec{r},t)$ can be expressed via complex amplitude $\vec{A}(\vec{r},t)$ and $s(\vec{r},t)$, respectively, according to the following equations:

$$\vec{E}(\vec{r},t) = \frac{1}{2}A(\vec{r},t)e^{i(k_0 z-\omega_0 t)}\hat{e}_x + c.c., \quad (2)$$

$$\vec{S}(\vec{r},t) = \frac{1}{2}S(\vec{r},t)e^{i(k_0 z-\omega_0 t)}\hat{e}_x + c.c.. \quad (3)$$

The amplitude of electric field is $A(r,z,\tau) = B(z,\tau)e^{i\psi(z,\tau)}e^{-(1-i\alpha)r^2/r_s^2}$, where $\tau = t - z/v_g$, v_g and $B(z,\tau)$ are group velocity and field's amplitude, respectively. Moreover $\Psi(z,\tau)$ corresponds to phase and $\alpha(z,\tau)$ represents the radius of curvature. Finally, $r_s(z,\tau)$ is the laser spot size. The source terms in the group velocity co-moving frame are as follows [4]:

$$S = (\frac{\omega_p^2}{c^2} - \frac{4}{r_{s0}^2})A(r,z,\tau). \quad (4)$$

The first term of source, corresponding to pre-formed parabolic plasma channel, demonstrates inhomogeneous density of plasma while second term indicates the finite transverse effect of the pulse. In equation (4), $\omega_p^2 = 4\pi n_e e^2/m$ and $n_e(r) = n_{e0} + n_{e0}\tan\left(\frac{z}{d}\right) + \frac{\Delta n_e r^2}{R_{ch}^2}$ in which density in the center of channel n_{e0}, Δn_e depth of channel, R_{ch} or channel's radius and d as a fixed parameter can be seen. Plasma profile density as a function of radius coordinate, and longitude coordinate of z in figure 1 is illustrated.

We utilize source-dependent expansion (SDE) method [4] to solve equation (1). As can be seen in below, integrals of source are used in this method:

$$F_{0,0}(z,\tau) = \frac{1}{2k_0}\int_0^{\infty} d\left(2\frac{r^2}{r_s^2}\right)S(r,z,\tau)e^{-(1+i\alpha(z,\tau))\frac{r^2}{r_s^2}}e^{-i\psi(z,\tau)} \quad (5-a)$$

$$F_{1,0}(z,\tau) = \frac{1}{2k_0}\int_0^{\infty} d\left(2\frac{r^2}{r_s^2}\right)S(r,z,\tau)\left(1 - 2\frac{r^2}{r_s^2}\right)e^{-(1+i\alpha(z,\tau))\frac{r^2}{r_s^2}}e^{-i\psi(z,\tau)}. \quad (5-b)$$

To obtain 4 coupled equations for amplitude of laser $B(z,\tau)$, phase $\Psi(z,\tau)$, the inverse of curvature's radius and spot size $r_s(z,\tau)$.

$$\frac{\partial\psi}{\partial z} = \frac{-2}{k_0 r_s^2} + \frac{2}{k_0 r_{s0}^2} - \frac{2\pi e^2 n_{e0}}{k_0 mc^2}\left(1 + \tan\left(\frac{z}{d}\right)\right), \quad (6)$$

$$\frac{\partial r_s}{\partial z} = \frac{2\alpha}{k_0 r_s}, \quad (7)$$

$$\frac{\partial\alpha}{\partial z} = \frac{2(1+\alpha^2)}{k_0 r_s^2} - \frac{2\pi e^2\Delta n_e}{k_0 mc^2}\cdot\frac{r_s^2}{R_{ch}^2}, \quad (8)$$

$$\frac{\partial B}{\partial z} = -\frac{2\alpha}{k_0 r_s^2}B. \quad (9)$$

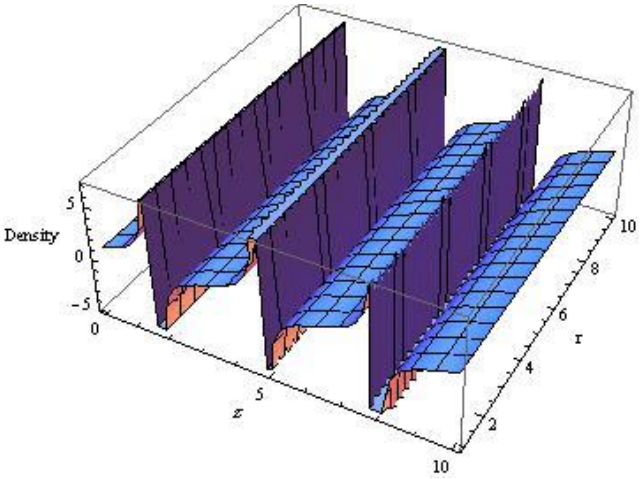

Fig. 1 Plasma density profile with radial and longitudinal variations in terms of radial coordinate r and longitudinal coordinate z.

To guide laser's pulse inside plasma channel, equation (6) to (9) should be zero. Equating equations (7) and (9) to zero, results in $\alpha=0$ and $B=cte$, which means that amplitude of laser and curvature of wave front inside channel remain unaffected. Finally, compatibility condition for guiding Gaussian beam with TEM_{00} mode, expressed below, can be obtained by equating equation (8) to zero.

$$r_s = \left(\frac{R_{ch}^2}{\pi r_e\Delta n_e}\right)^{1/4}, \quad (10)$$

$r_e = e^2/mc^2$ is classical radius of electron.

Coupled equations (6) to (9) can become dimensionless by using change of variables as follows:

$$\tilde{r}_s = \frac{r_s}{r_{s0}}, \qquad \frac{\partial}{\partial\tilde{z}} = Z_R\frac{\partial}{\partial z}, \qquad \tilde{n}_{e0} = \frac{n_{e0}}{N_n},$$

$$\Delta\tilde{n}_e = \frac{\Delta n_e}{N_n}, \quad \tilde{B} = \sqrt{\frac{n_0 c}{8\pi}}\sqrt{\frac{\pi r_{s0}^2}{2P_{in}}}B, \tag{11}$$

r_{s0}, Z_R, N_n, ω_0 and P_{in} are laser's spot size, Rayleigh length, density of neutral gas, and input power of laser, respectively. Therefore equations (5-8) are transformed into the following equations:

$$\frac{\partial\psi}{\partial\tilde{z}} = 1 - \frac{1}{\tilde{r}_s^2} - \frac{2\pi e^2 N_n Z_0 \tilde{n}_{e0}}{mc\omega_0}\left(1 + \tan\left(\frac{z_0\tilde{z}}{d}\right)\right), \tag{12}$$

$$\frac{\partial\tilde{r}_s}{\partial\tilde{z}} = \frac{\alpha}{\tilde{r}_s}, \tag{13}$$

$$\frac{\partial\alpha}{\partial\tilde{z}} = \frac{(1+\alpha^2)}{\tilde{r}_s^2} - \frac{2\pi e^2 N_n}{mc\omega_0}\cdot\frac{Z_0 r_{s0}^2}{R_{ch}^2}\Delta\tilde{n}_e\tilde{r}_s^2, \tag{14}$$

$$\frac{\partial B}{\partial z} = -\frac{\alpha}{\tilde{r}_s^2}\tilde{B}. \tag{15}$$

3 Numerical Results

In this section, we provide numerical solutions of unitless equations (12-15) which are obtained from Runge-Kutta method of order 4 (which we will explain in the next section) for Gaussian laser beam with incident wavelength $\lambda = 800$ nm. Figure 2 illustrates normalized laser pulse spot size r_s/r_{s0} as a function of normalized propagation distance z/z_0 in plasma channel for matched and mismatched modes. These line charts show that although the normalized laser spot size does not vary when the wave propagates inside plasma channel in the case of matched conditions, it oscillates periodically when matched conditions are not met.

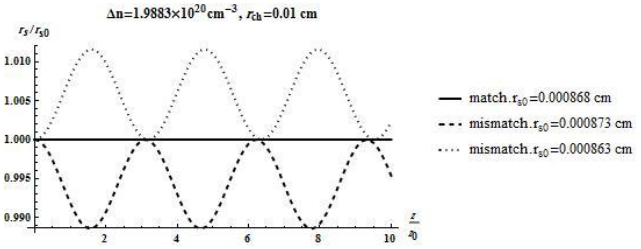

Fig. 2 Normalized spot size r_s/r_{s0} laser pulse in terms of normalized propagation distance z / z_0 during propagation in the plasma channel for matched and mismatched modes.

4 Runge-Kutta method

To show that the Rung-Kutta method of order 4 [11] can be applied to the equations (12) - (15), we write the dimensionless format of this equations as follows.

$$\dot{X}(z) = f(z, X(z)), \tag{16}$$

where

$$X(z) = \begin{bmatrix} x_1(z) \\ x_2(z) \\ x_3(z) \\ x_4(z) \end{bmatrix} = \begin{bmatrix} r_s(z) \\ \alpha(z) \\ B(z) \\ \psi(z) \end{bmatrix}, \tag{17}$$

$$f(z, X) = \begin{bmatrix} \frac{x_2}{x_1} \\ \frac{1+x_2^2}{x_1^2} - c_1 x_1^2 - c_2 x_3^2 \\ -\frac{x_2 x_3}{x_1^2} \\ 1 - \frac{1}{x_1^2} + c_3\left(1 + \tan\left(\frac{z_0 z}{d}\right)\right) \end{bmatrix}, \tag{18}$$

c_1, c_2 and c_3 are constants. According to Chapter 5 of [11], the 4th order Runge-Kutta method can be applied to well-posed systems. This means f must be continuous and satisfies a Lipschitz condition on its domain with Lipschitz constant $L < \infty$. Value of f satisfies the following inequality [12, 13]:

$$\left|\frac{\partial f}{\partial x_i}\right| \le L, \quad i = 1,2,3,4. \tag{19}$$

Now suppose

$$0 < m_1 = \min_{0\le z} x_1(z), M_i := \max_{0\le z} x_i(z), i = 1,2,3.$$

Then for the function f in (17) we have

$$\left|\frac{\partial f}{\partial x_1}\right| = \sqrt{\left(\frac{x_2}{x_1^2}\right)^2 + 4\left|c_1 x_1 + \frac{1+x_2^2}{x_1^2}\right|^2 + 4\left(\frac{x_2 x_3}{x_1^2}\right)^2 + \frac{4}{x_1^6}}$$
$$\le \sqrt{\left(\frac{M_2}{m_1^2}\right)^2 + 4\left|c_1 M_1 + \frac{1+M_2^2}{m_1^2}\right|^2 + 4\left(\frac{M_2 M_3}{m_1^2}\right)^2 + \frac{4}{m_1^6}}$$
$$=: L_1,$$

$$\left|\frac{\partial f}{\partial x_2}\right| = \sqrt{\left(\frac{1}{x_1}\right)^2 + 4\left|\frac{x_2}{x_1^2}\right|^2 + 4\left(\frac{-x_3}{x_1^2}\right)^2}$$

$$\leq \sqrt{\frac{1}{m_1^2} + 4\frac{M_2^2}{m_1^4} + \frac{M_3^2}{m_1^4}} =: L_2,$$

$$\left|\frac{\partial f}{\partial x_3}\right| = \sqrt{\left(\frac{-x_2}{x_1^2}\right)^2 + 4c_2^2 x_3^2} \leq \sqrt{\frac{M_2^2}{m_1^4} + 4c_2^2 M_3^2} =: L_3,$$

$$\left|\frac{\partial f}{\partial x_4}\right| = 0.$$

This means f has a Lipschitz condition with Lipschitz constant $L = \underset{i=1,2,3}{\text{Max}}\, L_i < \infty$ and since f continuous on its domain, then the system (15) is well posed.

5 Conclusions

In this paper, we investigated the Gaussian laser pulse guidance in the plasma channel numerically. It was assumed that the plasma channel's length and radius change over time. Matching conditions for guiding high intensity laser was also acquired. Using SDE method, the equations governing laser pulse parameters were solved by Runge-Kutta numerical method. Numerical results showed that in the case of matching condition, normalized laser spot size does not change. However, when these conditions are not met, the size of laser spot oscillate periodically.

References

1. S. Suckewer and C. H. Skinner, Comments At. Mol. Phys **30**, 331 (1995)
2. J. Zhou, J. Peatross, M. M. Murnane, H. C. Kapteyn, I. P. Christov Phys. Rev. Lett. **76**, 752 (1996)
3. T. Matsuoka, C. McGuffey, M. Levin, S. S. Bulanov, V. Chvykov, G. Kalintchenko, S. Reed, P. Rousseau, V. Yanovsky, A. Zigler, K. Krushelnick, A. Maksimchuk, Plasma Phys. Control. Fusion **51** (2009)
4. A. B. Borisov, A. V. Borovskii, V. V. Korobkin, A. M. Prokhorov, O. B. Shiriaev, X. M. Shi, T. S. Luk, A. McPherson, J. C. Solem, and K. Boyer, Phys. Rev. Lett. **68**, (1992)
5. C. E. Clayton, et al. Phys. Rev. Lett. **81**, 100 (1998)
6. T. Hosokai, M. Kando, H. Dewa, H. Kotaki, S. Kondo, K. Nakajima, K. Horioka, Opt. Lett. **25**, 10 (2000)
7. S. Jackel, R. Burris, J. Grun, A. Ting, C. Manka, K. Eans, J. Kosakowskii, Opt. Lett. **20**, 1086 (1995)
8. C. Courtois, B. Cros, G. Malka, G. Matthieussent, J. R. Marques, N. Blanchot, J. L. Miquel, J. Opt. Soc. Am. B: Opt. Phys. **17**, 864 (2000)
9. B. M. Luther, Y. Wang, M. C. Marconi, J. L. A. Chilla, M. A. Larotonda J. J. Rocca, Phys. Rev. Lett. **92** 23 (2004)
10. D. J. Spence, S. M. Hooker, Phys. Rev. E **63** (2000)
11. P. Sprangle, A. Ting, C. M. Tang, Phys. Rev. A **36** (1987)
12. R. L. Burden, J. D. Faires, *Numerical analysis* (7rd ed., Brooks-Cole, Pacific Grove, CA, 2001).
13. G. Birkhoff, G. Rota, *Ordinary differential equations*, (4th edition, New York: John Wiley and Sons, 1989).

TTMP vol 1(1), 2024
doi: 10.30511/TTMP.2023.709670

Transactions in Theoretical
and Mathematical Physics

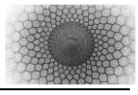

Spectrum Generating Algebra and its role in solvability of Alkali elements

H. Rahmati[a]

Department of Physics, Qom University of Technology,
Qom 37195-1519, Iran

Received: 13 March 2022/ Accepted: 15 December 2023/ Published: 05 February 2024

Abstract Hydrogen atom is always helpful in obtaining data from the other atoms. Revision of the Lie algebraic approach in studying the radial part of the Hydrogen atom and using the Tilting transformation are reasonable means to discuss Alkali elements. The characteristic difference between Alkali elements and Hydrogen atom is the screening effect in Alkali elements which causes much more freedom to the highest electron, valence electron. In this case, these atoms have another terms besides coulomb potential energy; Sentences of the order of inverse square of the distance and above. So, we can consider we have dipole moments, quadruple moments and etc. Therefore, these terms , although they are small, make these elements attractive for applications in quantum information. Also, we can consider them as Rydberg atoms with strong long-range interactions. Here, by considering an inverse square distance potential, Lie algebraic methods help us to obtain energy levels of both bound and excited states and corresponding wave functions too.

1 Introduction

Many physical systems with hidden symmetry in their Hamiltonian are solvable algebraically [1].Keplerian problems with central 2-body potentials, such as Hydrogen-like atoms with Coulomb potential in the non-relativistic: Schrodinger type, or relativistic: Klein-Gordon (K-G) or Dirac types, are some examples [2-5].

On the other hand, using Lie algebraic approach in solving physics problems is custom. Applying the generators of a Lie algebra, Γ_j, one could write the general form of the exact solvable or quasi-exact solvable (QES) Hamiltonian operator as follows [6-7]:

$$H = \sum_{j,k}^{n} C_{jk}\Gamma_j\Gamma_k + \sum_{j=1}^{n} C_j\Gamma_j. \tag{1}$$

Here C_{jk},C_j are coefficients can be found by comparing (1) with the physical Hamiltonian. This Lie algebra is called spectrum generating algebra (SGA), widely used in compact and finite dimensional Lie algebras [8-9]. However, following mathematical tricks, one could extend this method to the non-compact and infinite dimensional Lie algebras too [10-11].

For two reasons, we mainly focus on the Lie algebra $so(2,1)$: firstly, the Tilting transformation is an appropriate proposition in this Lie algebra; then, this Lie algebra is suitable for studying Hydrogen-like atoms such as Alkali elements. To illustrate Tilting transformation in this case, first, one should ,rewrites the Hamiltonian in terms of the generators of Lie algebra $so(2,1)$. Then, a rotation by an angle θ, Tilting angle, can be exerted to take the spectrum of bound and scattering states [12].

Another aspect of Alkali elements is the existence of valence electron makes these atoms Rydberg atoms. Rydberg atoms are those in which the valence electron is in the state of high principal quantum number n. They are of historical interest because of their role in atomic spectroscopy [13] since 1970. The exaggerated properties of Rydberg atoms allow doing experiments that would be difficult or impossible with normal atoms. In this case, applying experimental methods of laser cooling and spectroscopy can be used to study their properties. One of the recent studies of Rydberg atoms has been made by Ryabtsev and his collaborators in the case of Rb element and its role in quantum information [14].

On the other hand, lots of the information from Hydrogen atom is helpful to study Hydrogen-like atoms such as Alkali elements. However, the point is that the valence electron is

[a]e-mail: hrahmati1357@yahoo.com

not attracted by nuclear charge Ze, but by a smaller charge than Ze. The electrons in the lower levels of the atom screen the nuclear charge; So, the charge of nuclear decreases to $Z'e = (Z-\mu)e$, where μ is the coefficient of screening effect for any Alkali elements. It is obvious that the valence electron in this case has much more freedom to the other electrons of the atom. Therefore, in a simple model, one can consider the Alkali elements as Rydberg atoms.
Here, in section 2, we review the Lie algebraic investigations of the Hydrogen atom. After that in sec.3, the extension of these results to the Alkali elements by considering the screening effect as an inverse square distance relation is demonstrated. Also, by using SGA in the case of new Lie algebra $so(2,1)$, we obtain the spectrum of Alkali elements in two cases: bound states and scattering states. Finally, in sec.4 the conclusion and discussion are presented.

2 Review of so(2,1) Lie algebraic method in Hydrogen atom

Hamiltonian of Hydrogen atom is:

$$H = \frac{P^2}{2m_e} - k\frac{e^2}{r}, \tag{2}$$

where: m_e (electron mass), r (distance from nuclear to valence electron), P (momentum), e (charge of electron) and k (Coulomb constant). Since, the Coulomb potential is radial, the Hamiltonian is solvable in the spherical polar system and the radial part of it, namely,

$$r(H-E)|R(r)>=\Pi|R(r)>=0, \tag{3}$$

is

$$(r\frac{d^2}{dr^2}+2\frac{d}{dr}-\frac{l(l+1)}{r^2}+(ke^2-Er)\frac{2m_e}{\hbar^2})R(r)=0. \tag{4}$$

For simplicity, we work in the atomic units (a.u.) where we have $e=\hbar=k=m_e=1$. The parameter $l(l+1)$ is the eigenvalue of the angular momentum operator [15]. This solvable equation could be written by the generators of $so(2,1)$ Lie algebra:

$$\begin{aligned}
\Gamma_1 &= \frac{1}{2}(rP^2+r-a\frac{\alpha^2}{r}-bi\alpha\frac{\vec{\gamma}.\vec{r}}{r^2}),\\
\Gamma_2 &= \frac{1}{2}(rP^2-r-a\frac{\alpha^2}{r}-bi\alpha\frac{\vec{\gamma}.\vec{r}}{r^2}),\\
\Gamma_3 &= \vec{r}.\vec{P},
\end{aligned} \tag{5}$$

and commutation relations:

$$[\Gamma_1,\Gamma_2]=i\Gamma_3,\ \ [\Gamma_2,\Gamma_3]=-i\Gamma_1,\ \ [\Gamma_3,\Gamma_1]=i\Gamma_2. \tag{6}$$

Table 1 Coefficients of the equation (8) in three cases

Coefficients	Schrodinger	K-G	Dirac
C_1	$\frac{1}{2m}$	1	1
C_2	$-E$	$-(E^2-{E_0}^2)$	$-(E^2-{E_0}^2)$
C_3	$-\alpha$	$-2\alpha E$	$-2\alpha E$

Here a,b are constant parameters and $\alpha=\frac{e^2}{\hbar c}=7.29\times10^{-3}$ is the fine structure constant and $\gamma_i=\begin{pmatrix}0 & \sigma_i\\ \sigma_i & 0\end{pmatrix}$ in which σ_i are the Pauli matrices. Following Eq.(1) general Hamiltonian of $so(2,1)$ Lie algebra is:

$$\Pi = C_1\Gamma_1+C_2\Gamma_2+C_0. \tag{7}$$

This is a second order differential equation and hermitian operator. It is obviously possible to write

$$\Pi = C_1(\Gamma_1+\Gamma_2)+C_2(\Gamma_1-\Gamma_2)+C_0. \tag{8}$$

Choosing an appropriate expression for C_1,C_2 and C_0 we obtain the Hamiltonians both in the non relativistic and relativistic cases. If we have $a=b=0$ Eq.(8) is the non relativistic Schrodinger equation of Hydrogen atom. For $a=1,b=0$ Eq.(8) concludes K-G and by substitution $a=b=1$ we have the second order Dirac equation [5].

The casimir operator of this Lie algebra is:

$$C^2=\Gamma_3^2-\Gamma_1^2-\Gamma_2^2=-a\alpha^2-b\alpha. \tag{9}$$

This operator has a negative sign, which means the non-compactness character of $so(2,1)$ Lie algebra. On the other hand, the radial wave function $R(r)=|\Psi\rangle$ depends on two quantum numbers n,l and is independent of angular momentum orientation; i.e., it is invariant under rotation. Therefore, we could establish Tilting transformation for solving Eq.(8), written by the generators of $so(2,1)$ Lie algebra. In this transformation Γ_1,Γ_2 generators are rotated by an angle θ around the operator Γ_3, which does not appear in the radial Hamiltonian (8):

$$e^{i\theta\Gamma_3}(\Gamma_1\pm\Gamma_2)e^{-i\theta\Gamma_3}=e^{\pm\theta}(\Gamma_1\pm\Gamma_2), \tag{10}$$

and the transformed wave function $|\widetilde{\Psi}\rangle=e^{i\theta\Gamma_3}|\Psi\rangle$; Following these receptions, the eigenvalue equations $\Pi|\widetilde{\Psi}\rangle=0$ for any suitable angle θ conclude the spectrum of bound states and scattering states [16].

3 so(2,1) Lie algebra and SGA in Alkali elements

One of the most traditional methods of using Lie algebra in physics is that the Hamiltonian and other physical operators could be written in terms of the generators of this Lie algebra. In this case, this Lie algebra is called SGA [1]. But,

sometimes, all of the generators do not appear in the algebraic form of the Hamiltonian, whereas all of them are in the Casimir operator. In this case, we can obtain the spectrum using a unitary transformation and then rotating the Hamiltonian by an angle θ around the missing generator. This trick concludes the solvability of the system.
Interaction of an electron with an electromagnetic field, i.e., $(\overrightarrow{E},\overrightarrow{B})$, the ordinary atom, can be expressed in terms of the Lie algebra $so(4,2)$. The operators of this Lie algebra are [5]:

$$\overrightarrow{J}=\overrightarrow{r}\times\overrightarrow{P},\quad \overrightarrow{M}=\frac{1}{2m}(\overrightarrow{P}\times\overrightarrow{L}-\overrightarrow{L}\times\overrightarrow{P})-\frac{Ze^2}{r^2}\overrightarrow{r}$$
$$\overrightarrow{A}=\frac{1}{2m}(\overrightarrow{P}\times\overrightarrow{L}-\overrightarrow{L}\times\overrightarrow{P})+\frac{Ze^2}{r^2}\overrightarrow{r},\quad A_4=\overrightarrow{r}.\overrightarrow{P}-\frac{3}{2}i\hbar,$$
$$\Gamma_i=rP_i,\quad \Gamma_4=\frac{1}{2}(r\overrightarrow{P}.\overrightarrow{P}-r),\quad \Gamma_5=\frac{1}{2}(r\overrightarrow{P}.\overrightarrow{P}+r). \qquad (11)$$

However, some of these operators are needed in the radial equation of Alkali elements with screening effect. In fact, only A_4,Γ_4 and Γ_5 by adding a new term are sufficient. In this case, the effective potential energy for (valence electron)+(nuclear+rest of the electrons) is:

$$U_{eff}=-\frac{Z}{r}+\frac{l(l+1)}{2r^2}+\frac{\mu}{2r^2}. \qquad (12)$$

By summarizing two terms 2,3 as follows:

$$l(l+1)+\mu=l'(l'+1). \qquad (13)$$

The quantum level l goes up to l' where $l'>l$:

which means the freedom of the valence electron is now more than the other electrons of atom. Also, we see from table.2 that by increasing the atomic number of Alkali elements, this effect is much series. In this case, the generators of $so(2,1)$ Lie algebra become:

$$\Gamma_1=\frac{1}{2}(rP^2+r+\frac{l'(l'+1)}{r}),$$
$$\Gamma_2=\frac{1}{2}(rP^2-r+\frac{l'(l'+1)}{r}),$$
$$\Gamma_3=\vec{r}.\vec{P}. \qquad (14)$$

Therefore, in the case of relativistic Hamiltonian of $so(2,1)$ Lie algebra by using Eq.(8) and table 1:

$$\Pi|\Psi(r)\rangle=$$
$$[(\Gamma_1+\Gamma_2)-(E^2-E_0^2)(\Gamma_1-\Gamma_2)-2\alpha ZE]|\Psi(r)\rangle=0. \qquad (15)$$

If we work in the center of mass system, we should consider reduced mass m_{red}:

$$m_{red}=\frac{Mm_e}{M+m_e}\simeq 1, \qquad (16)$$

and for the rest energy in a.u. we have:

$$E_0=m_{red}c^2=\frac{1}{\alpha^2}. \qquad (17)$$

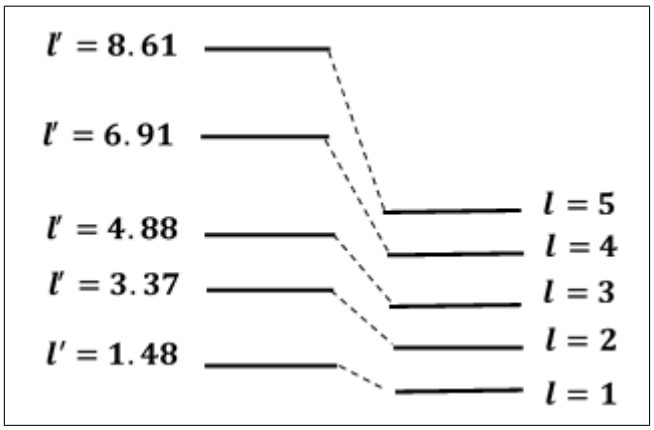

Fig. 1 Comparing the level of valence electron without and with the screening effect

Now, by using Tilting transformation

$$[(e^{-\theta}-(E^2-\frac{1}{\alpha^4})e^{\theta})\Gamma_1+$$
$$(e^{-\theta}+(E^2-\frac{1}{\alpha^4})e^{\theta})\Gamma_2-2\alpha ZE]|\widetilde{\Psi}(r)\rangle=0, \qquad (18)$$

the generators Γ_1,Γ_2 obey:

$$\Gamma_1|N,l\rangle=N'|N,l\rangle,\quad \Gamma_2|N,l\rangle=\lambda|N,l\rangle, \qquad (19)$$

where $N'=N+l'+1$ is real and discrete value, whereas λ is imaginary and continues value. The rotation angle θ must be chosen for the bound states to eliminate the non-compact generator Γ_1, so that $e^{-\theta}=k=\pm\sqrt{-(E^2-\frac{1}{\alpha^4})}$ and:

$$E=\frac{-N'}{\alpha^2\sqrt{N'^2+Z^2\alpha^2}},$$
$$\Psi(r)=e^{-\theta}\sqrt{\frac{2r}{N'^3}}\bigwedge_{N'-l'-1}^{2l'+1}(\frac{2r}{N'}), \qquad (20)$$

where $\bigwedge_n^l(r)$ is the generalized Laugurre function [17]. If we choose $e^{-\theta}=K=\pm\sqrt{E^2-\frac{1}{\alpha^4}}$, so that the compact generator Γ_2 can be eliminated:

$$E=\frac{\lambda}{\alpha^2\sqrt{\lambda^2+Z^2\alpha^2}},$$
$$\Psi(r)=\frac{e^{-\theta}}{r}\sqrt{\frac{2}{\pi}}\sin(Kr-\frac{\pi}{2}l'+\frac{Z\alpha}{K}(\log(2Kr)+\delta(l'))), \qquad (21)$$

where $\delta(l')=arg(\Gamma(l'+1-i\frac{Z\alpha}{K}))$ and $\Gamma(l)$ shows Gamma function[18].

Table 2 Some of the quantum numbers of Alkali elements

Alkali elements	l	Z	μ	l'	Z'	$\Delta l'$
Li	1	3	1.7	0.68	1.3	0.32
Na	2	11	8.8	0.86	2.9	1.14
K	3	19	16.8	1.46	2.9	1.54
Rb	4	37	34.8	1.18	2.9	2.82
Cs	5	55	52.8	1.46	2.9	3.54

4 Conclusion and Discussion

The radial part of the Hydrogen atom is solvable algebraically in both non-relativistic and relativistic cases. The underlying Lie algebra is $so(2,1)$. Typically, this part of the Hamiltonian for specified angular momentum l is only dependent on the principal quantum number n and this is the reason for using Tilting transformation. Using this method, we could obtain the spectrum of bound states and scattering states for a certain angle θ. Here we extend this method to Alkali elements which are Hydrogen-like and we see that by considering the screening effect as an inverse square distance potential, we obtain the new expression for the principal quantum number in bound states and a new term in the scattering phase shift.

Actually, the screening effect causes the Alkali element to be considered as a dipole moment where its negative charge is the valence electron and the positive part of it is the (nuclear+rest electrons of the atom). This pattern is similar to Rydberg atoms, which we consider here for Alkali elements.

References

1. F. Iachello, *Lie algebras and applications*, (Springer verlag Berlin, 2006)
2. A. Bohm, *Quantum Mechanic*, (Springer verlag Berlin, 1979)
3. A. O. Barut and G. L. Bornzin, J. Math. Phys. **12**, 841 (1971)
4. S. Kais and S. K. Kim, Physics Letter **114A**, 165 (1986)
5. R. Gilmore, *Lie Groups, Physics and Geometry* (John Wiley and sons, 2006)
6. M. A. Shifman, A. V. Turbiner, Commun. Math. Phys **126**, 347 (1989)
7. A. G. Lopez, N. Kamran, P. J. Olver, Contem. Math. **160**, 113 (1994)
8. F. Iachello, A. Arima, *The Interacting Boson Model* (Cambridge Press, Cambridge, 1987)
9. F. Iachello, R. Levine, *Algebraic Theory of Molecules* (Oxford Press, Oxford, 1995)
10. Y. Alhassid, F. Gursey, F. Iachello, Phys. Rev. Lett. **50** (1983)
11. Y. Alhassid, F. Gursey, F. Iachello, Ann. Phys. **148** (1983)
12. A. Frank, K. B. Wolf, Phys. Rev. Lett. **52** (1984)
13. G. Drake, *Springer Handbook of Atomic, Molecular, and Optical Physics* (Springer-Verlag New York, 2006)
14. I.I. Ryabtsev, I.I. Beterov, D.B.Tretyakov, V.M. Entin, E.A. Yakshina, Physics.Uspekhi **2**, 59 (2016)
15. J. J. Sakurai, *Modern Quantum Mechanics* (Addison-Wesley, 1985)
16. A. Alhaidari, Phys. Lett. A. **322**, 72 (2004)
17. R. L. Liboff *Introductory Quantum Mechanics* (Addison-Wesley, 1993)
18. L. D. Landau, E. M. Lifshitz, *Quantum mechanics, Non relativistic theory* (second Ed. vol 3, Pergamon Press, 1974)

TTMP vol 1(1), 2024
doi: 10.30511/TTMP.2024.709742

Transactions in Theoretical and Mathematical Physics

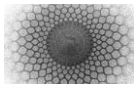

Numerical–Fitting–Nikiforov–Uvarov method applied to Schrödinger Equation

A. Niknam[1], A. A. Rajabi[1], M. Solaimani[a,2]
[1] Physics Faculty, Shahrood University, P.O. Box 3619995161-316 Shahrood, Iran
[2] Department of Physics, Qom University of Technology, Qom, Iran

Received: 04 July 2022/ Accepted: 30 December 2023/ Published: 05 February 2024

Abstract In this work, we have solved the radial Schrödinger equation for the Woods–Saxon potential together with coulomb (r>Rc), centrifugal terms and spin-orbit interaction by using a new type of Nikiforov-Uvarov (NU) method. This approach is based on the Second-Order Linear Differential Equations (SOLDE) solution. The mandatory specific choices of the required parameters in this technique restrict the application of this method to the Schrödinger equation with complicated potential profiles, which means that the NU method cannot efficiently be employed to solve more realistic physical systems. Due to the mentioned difficulties in evaluating the equivalent second-order algebraic equation in the NU method, the analytical NU method has to be extended to the more efficient version combined with numerical methods (that leads to a semi-analytical method). We have solved it by combining the NU method with the numerical fitting schema. The numerical fitting schema helps us find the mentioned second-order algebraic equation. Otherwise, complicated changes of variables or overwhelming algebraic treatments to derive the energy eigenvalues and the wavefunctions are required. The current approach is simpler, more flexible and efficient. This technique can also be developed for equations other than the Schrodinger one. The Woods–Saxon potential is also a short-range interaction in the potential model for nuclear physics and has predictions for the nuclear shell model and distribution of nuclear densities. We have obtained semi-analytical energy eigenvalues and eigenfunctions for various values of n, l, and j quantum numbers. Agreement of $5/2^+$ and $1/2^+$ wavefunctions with the published works is also obtained, showing the accuracy of our method.

1 Introduction

The asymptotic giant branch [1] is an evolutionary phase through which many stars, including the Sun, eventually pass. This phase involves a hydrogen and a helium shell that burns alternately, surrounding an inactive stellar core. The $^{16}O(p, \gamma)^{17}F$ reaction rate sensitively influences the $^{17}O/16O$ isotope predicted by models of massive stars, where proton captures occur at the base of the convective envelope. In the study of the breakup of ^{17}F into proton + ^{16}O, some potential models for 17F have been used previously, such as Woods–Saxon Potential with Spin-Orbit and Coulomb potentials [2] and M3Y interaction model [3]. The solution of the Schrödinger equation, including the above potentials, has been done using the numerical methods in the above-mentioned works. This is because the analytical solution of these equations is not possible. However, some theoretical groups have tried to solve these Schrödinger equations analytically. For example, Pahlavani et al. solved the Schrödinger equation, including Woods–Saxon Potential with Spin-Orbit and Centrifugal Terms by Nikiforov–Uvarov Method [4]. They did not include the coulomb term in their calculations. Adding the coulomb potential (here for r<Rc; Rc= spherical nucleus radius) and the solution of the Schrödinger equation by the Nikiforov–Uvarov Method is the main goal of the present work. Our previous works used the NU method to solve the Schrödinger equation with different potentials. Energy-dependent potential [5] and angle-dependent potential [6] are two. We have also solved the Dirac equation with the NU method, including Hartmann Potential [7], Duffin–Kemmer–Petiau (DKP) equation with Woods–Saxon Potential [8] and Hulthen vector potential [9] and Klein–Gordon equation with Energy-Dependent Potential [10]. We have solved the Schrödinger equation in the presence of the spin-orbit interaction, Woods–Saxon potential together with coulomb (r>Rc) and centrifugal terms by a combination of the numerical fitting and NU methods and obtained energy eigenvalues and corresponding eigenfunctions.

2 Parametric NU method

This powerful mathematical tool could be used to solve

* Corresponding author
[a] solaimani.mehdi@gmail.com

the second-order differential equations. Considering the following differential equation [10–12]

$$\psi_n''(s)+\frac{\tilde{\tau}(s)}{\sigma(s)}\psi_n'(s)+\frac{\tilde{\sigma}(s)}{\sigma(s)^2}\psi_n(s)=0, \quad (1)$$

Where $\sigma(z)$ and $\tilde{\sigma}(z)$ are polynomials of second order at most, and$\tilde{\tau}(z)$ is a first-order polynomial. To make the application of the NU method simpler and the checking of the validity of the solution unnecessary, we present a shortcut for the method. We begin the method by writing the general form of the Schrodinger-like equation (1) as

$$\psi_n''(s)+\left(\frac{c_1-c_2 s}{s(1-c_3 s)}\right)\psi_n'(s)+\left(\frac{-p_2 s^2+p_1 s-p_0}{s^2(1-c_3 s)^2}\right)\psi_n(s)=0, \quad (2)$$

where the wave functions satisfy

$$\psi_n(s)=\phi(s)y_n(s). \quad (3)$$

By comparing Eq. (3) with its counterpart Eq. (2), one can obtain

$$\tilde{\tau}(s)=c_1-c_2 s, \quad \sigma(s)=s(1-c_3 s),$$
$$\tilde{\sigma}(s)=-p_2 s^2+p_1 s-p_0, \quad (4)$$

According to the NU method [10], one can obtain the bound state energy equation as [11, 12]

$$c_2 n-(2n+1)c_5+(2n+1)\left(\sqrt{c_9}+c_3\sqrt{c_8}\right)+n(n-1)c_3+c_7+2c_3c_8+2\sqrt{c_8c_9}=0, \quad (5)$$

where,

$$c_4=\frac{1}{2}(1-c_1), \quad (6-1)$$

$$c_5=\frac{1}{2}(c_2-2c_3), \quad (6-2)$$

$$c_6=c_5^2+p_2, \quad (6-3)$$

$$c_7=2c_4c_5-p_1, \quad (6-4)$$

$$c_8=c_4^2+p_0, \quad (6-5)$$

$$c_9=c_3(c_7+c_3c_8)+c_6, \quad (6-6)$$

$$c_4=\frac{1}{2}(1-c_1). \quad (6-7)$$

In addition, we also find that:

$$\rho(s)=s^{c_{10}}(1-c_3 s)^{c_{11}}, \quad (7-1)$$

$$\varphi(s)=s^{c_{12}}(1-c_3 s)^{c_{13}}, \quad (7-2)$$

$$c_{12}>0, c_{13}>0, \quad (7-3)$$

$$y_n(s)=P_n^{(c_{10},c_{11})}(1-2c_3 s), c_{10}>-1, c_{11}>1, \quad (7-4)$$

are necessary in calculating the wave functions.

$$\psi_{nl}(s)=N_{nl}s^{c_{12}}(1-c_3 s)^{c_{13}}P_n^{(c_{10},c_{11})}(1-2c_3 s), \quad (8)$$

where, $P_n^{(\mu,\nu)}(x), \mu>1, \nu>1, x\in[-1,1]$ are Jacobi polynomials. All undefined constant parameters are as follows [13],

$$c_{10}=c_1+2c_4+2\sqrt{c_8}, \quad (9-1)$$

$$c_{11}=1-c_1-2c_4+\frac{2}{c_2}\sqrt{c_9}, \quad (9-2)$$

$$c_{12}=c_4+\sqrt{c_8}, \quad (9-3)$$

$$c_{13}=-c_4+\frac{1}{c_3}\left(\sqrt{c_9}+c_5\right), \quad (9-4)$$

where $c_3\neq 0$, $c_{13}>0$, $c_{12}>0$, $s\in\left[\frac{1,1}{c_{13}}\right]$ and $c_{13}\neq 0$.

3 Solutions of Schrödinger Equation

We start with the radial part of the Schrödinger equation as,

$$\frac{d^2R(r)}{dr^2}+\frac{2\mu}{\hbar^2}\left[E-V(r)-\frac{\hbar^2 l(l+1)}{2\mu r^2}\right]R(r)=0. \quad (10)$$

The potential profile contains the following terms:
1- woods-saxon term:

$$V_{ws}=\frac{-V_0}{1+e^{\frac{(r-R_0)}{a}}}, \quad (11)$$

were we have used $V_0=42.77MeV$ for ^{17}F atoms.
2- spin-orbit term:

$$V_{LS}(r)=\frac{1}{2}V_{LS}^{(0)}\left(\frac{r_0}{\hbar}\right)^2\frac{1}{r}\left[\frac{d}{dr}\frac{1}{1+e^{\frac{(r-R_0)}{a}}}\right](\vec{L}.\vec{S}), \quad (12)$$

where we have used $V_{LS}^{(0)}=0.44V_0$.
3- Coulomb term:

$$V_C(r) = \begin{cases} \frac{e^2}{\pi\varepsilon_0 R_C}\left[3 - \left(\frac{r}{R_C}\right)^2\right] & r \le R_C \\ \frac{8e^2}{4\pi\varepsilon_0 r} & r > R_C \end{cases} . \quad (13)$$

Here we have solved the Schrödinger equation for r>R_c. By using the change of variable as $\psi(r) = rR(r)$ we have,

$$\frac{d\psi}{dr} = R(r) + r\frac{dR(r)}{dr}. \quad (14)$$

Then the Schrödinger equation becomes

$$\frac{d^2\psi(r)}{dr^2} + \frac{2\mu E}{\hbar^2}\psi(r) - \frac{2\mu V(r)}{\hbar^2}\psi(r) - \frac{l(l+1)}{r^2}\psi(r) = 0. \quad (15)$$

Now, the complete Schrödinger equation reads,

$$\frac{d^2\psi(r)}{dr^2} + \frac{2\mu}{\hbar^2}\left[E - \frac{-V_0}{1+e^{\frac{(r-R_0)}{a}}} - \frac{1}{2}V_{LS}^{(0)}r_0^2\frac{1}{r}\left(\frac{d}{dr}\frac{1}{1+e^{\frac{(r-R_0)}{a}}}\right)\left(j(j+1) - l(l+1) - \frac{3}{4}\right) - \frac{1}{4\pi\varepsilon_0}\frac{8e^2}{r}\right]\psi(r) - \frac{l(l+1)}{r^2}\psi(r) = 0. \quad (16)$$

We need another change of variable, which leads to

$$\frac{d\psi(r)}{dr} = \frac{d\psi(r)}{ds} \times \frac{ds}{dr} = -\delta s\frac{d\psi(r)}{ds}, \quad (17-1)$$

$$\frac{d^2\psi(r)}{dr^2} = \delta^2 s^2\frac{d^2 R(s)}{ds^2} + \delta^2 s\frac{dR(s)}{ds}. \quad (17-2)$$

We define $\delta = \frac{1}{a}$, $q = e^{\delta R_0}$, $V_0' = V_0 q$ and $V'^0_{LS} = V^0_{LS} q$. We have also used the following approximation:

$$\frac{1}{r^2} \approx \delta^2\left(\frac{e^{-\delta r}}{1-e^{-\delta r}}\right)^2. \quad (18)$$

To find the best value of the δ we have changed the δ and plotted both side of the above equation several times and found the best δ to be 0.4fm^{-1}. Figure (1) shows two sides of the above equation to obtain δ. By using the later change of variable, the Schrödinger equation reads,

$$\delta^2 s^2\frac{d^2R(s)}{ds^2} + \delta^2 s\frac{dR(s)}{ds} + \left(\frac{2\mu E}{\hbar^2} + \frac{2\mu V_0'}{\hbar^2}\right)\left(\frac{s}{1+qs}\right) + \frac{\mu\delta^2 r_0^2 V'^0_{LS}}{\hbar^2}\left(j(j+1) - l(l+1) - \frac{3}{4}\right)\frac{s^2}{(1-s)(1+qs)^2} - \frac{4\mu e^2\,\delta}{\pi\hbar^2\,\varepsilon_0}.\frac{s}{1-s} - l(l+1)\frac{\delta^2 s^2}{(1-s)\hat{}2)}R(s) = 0. \quad (19)$$

After some simplifications we have

$$\frac{d^2R(s)}{ds^2} + \frac{1}{s}\frac{dR(s)}{ds} + \left(\frac{\frac{2\mu E}{(\hbar^2\delta^2)(1-s)^2} + \frac{2\mu V_0'}{\hbar^2\delta^2}\frac{s(1-s)^2}{(1+qs)}}{s^2(1-s)^2} + \frac{\frac{\mu r_0^2 V'^0_{LS}}{\hbar^2}\left(j(j+1) - l(l+1) - \frac{3}{4}\right)\frac{s^2(1-s\quad)}{(1+qs)^2}}{s^2(1-s)^2} - \frac{\frac{4\mu e^2}{\pi\varepsilon_0\hbar^2\delta}s(1-s\quad) - l(l+1)s^2}{s^2(1-s)^2}\right)R(s) = 0. \quad (20)$$

In order to use the N-U method we have to convert the numerator of the potential term to a second order polynomial For this purpose, we have used the following approximations,

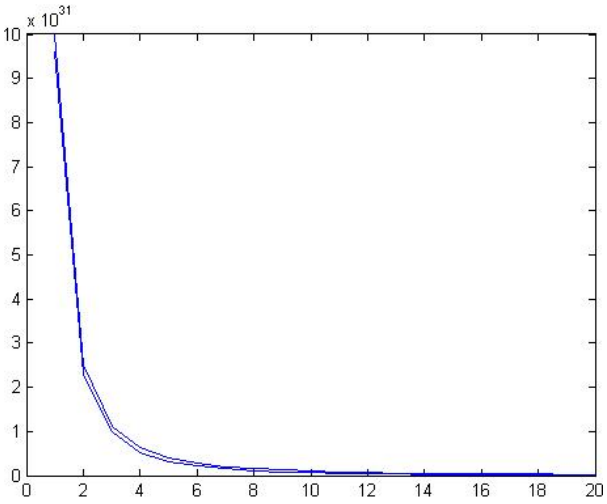

Fig. 1 Left hand side and Right hand side of the equation (3-1) to obtain δ.

$$\frac{s(1-s[\quad]^2]}{1+qs} = 0.006595579s^2 - 0.0132710857s + 0.0067413175, \quad (21)$$

which has been obtained through numerical fitting schema. Figure (2) shows the two sides of the equation above.

As it is clear, this approximation is extremely good. We have also used from:

$$\frac{s^2(1-s\quad)}{(1+qs)^2} = -3.3579988\times10^{-9}s^2 - 0.432019240084\times10^{-4}s + 0.4341808999\times10^{-4}, \quad (22)$$

which has been obtained through numerical fitting schema. Figure (3) shows the two sides of the equation above.

As it is clear, this approximation is extremely good. In order to convert the last Schrödinger equation to the N-U type Schrödinger equation,

$$\psi_n''(s)+\frac{\tilde{\tau}(s)}{\sigma(s)}\psi_n'(s)+\frac{\tilde{\sigma}(s)}{\sigma(s)^2}\psi_n(s)=0, \qquad (23)$$

$$\psi_n''(s)+\left(\frac{1-s}{s(1-s)}\right)\psi_n'(s)+\left(\frac{-\gamma s^2+\beta s-\varepsilon^2}{s^2(1-s)^2}\right)\psi_n(s)=0, \qquad (24)$$

We define three parameters $\varepsilon, \beta, \gamma$ as follows,

$$-\gamma=\frac{2\mu E}{\hbar^2\delta^2}+\frac{2\mu V_0'}{\hbar^2\delta^2}(0.006595579)-\left(\frac{\mu V'^{(0)}_{LS} r_0^2\left(j(j+1)-l(l+1)-\frac{3}{4}\right)}{\hbar^2}\right)\times 3.3579988\times 10^{-9}+\frac{4\mu e^2}{\pi\varepsilon_0\hbar^2\delta}-l(l+1), \qquad (25-1)$$

$$\beta=-\frac{4\mu E}{\hbar^2\delta^2}-\frac{2\mu V_0'}{\hbar^2\delta^2}(0.0132710857)-\frac{\mu V'^{(0)}_{LS} r_0^2\left(j(j+1)-l(l+1)-\frac{3}{4}\right)}{\hbar^2}\times(0.432019240084\times 10^{-4})-\frac{4\mu e^2}{\pi\varepsilon_0\hbar^2\delta}. \qquad (25-2)$$

Now we write the β,γ as function of ε:

$$-\gamma=\frac{2\mu E}{\hbar^2\delta^2}+\frac{2\mu V_0'}{\hbar^2\delta^2}(0.006595579)-\frac{\mu V'^{(0)}_{LS} r_0^2\left(j(j+1)-l(l+1)-\frac{3}{4}\right)}{\hbar^2}\times(3.3579988.10^{-9})+\frac{4\mu e^2}{\pi\varepsilon_0\hbar^2\,\delta}-l(l+1), \qquad (26-1)$$

$$\beta=-\frac{4\mu E}{\hbar^2\delta^2}-\frac{2\mu V_0'}{\hbar^2\delta^2}(0.0132710857)-\frac{\mu V'^{(0)}_{LS} r_0^2\left(j(j+1)-l(l+1)-\frac{3}{4}\right)}{\hbar^2}\times(0.432019240084.10^{-4})-\frac{4\mu e^2}{\pi\varepsilon_0\hbar^2\,\delta}, \qquad (26-2)$$

$$-\varepsilon^2=\frac{2\mu E}{\hbar^2\delta^2}+\frac{2\mu V_0'}{\hbar^2\delta^2}(0.0067413175)+\frac{\mu V'^{(0)}_{LS} r_0^2\left(j(j+1)-l(l+1)-\frac{3}{4}\right)}{\hbar^2}\times(0.4341808999.10^{-4}). \qquad (26-3)$$

Now we write the β,γ as function of ε,

$$\gamma=\varepsilon^2+\frac{\mu V_0'}{\hbar^2\delta^2}(0.000291477)+\frac{\mu V'^{(0)}_{LS} r_0^2\left(j(j+1)-l(l+1)-\frac{3}{4}\right)}{\hbar^2}\times(0.434214479888\times 10^{-4})-\frac{4\mu e^2}{\pi\varepsilon_0\hbar^2\delta}+l(l+1)\rightarrow\gamma=\varepsilon^2+A, \qquad (27-1)$$

$$\beta=2\varepsilon^2+\frac{\mu V_0'}{\hbar^2\delta^2}(0.0004230986)+\frac{\mu V'^{(0)}_{LS} r_0^2\left(j(j+1)-l(l+1)-\frac{3}{4}\right)}{\hbar^2}\times(0.436342559716\times 10^{-4})-\frac{4\mu e^2}{\pi\varepsilon_0\hbar^2\delta}\rightarrow\beta=2\varepsilon^2+B, \qquad (27-2)$$

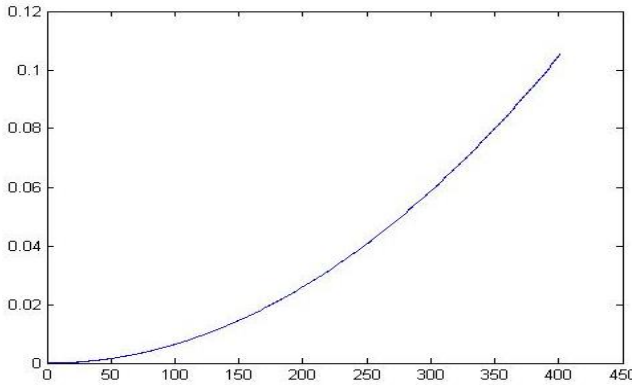

Fig. 2 left hand side and right-hand side of the equation (3-2) to show the accuracy of this approximation.

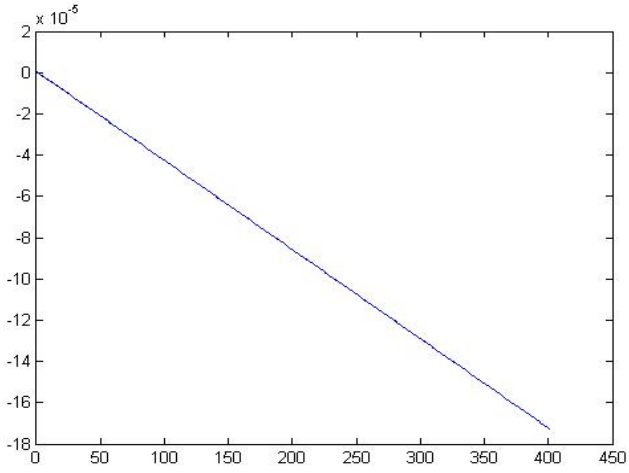

Fig. 3 Left hand side and right hand side of the equation (3-3) to show the accuracy of this approximation

Based on what we have described above in the N-U section, we can find the following second order polynomial,

$$\mathrm{n}-(2\,\mathrm{n}+1)\left(-\frac{1}{2}\right)+(2\,\mathrm{n}+1)\left(\sqrt{\gamma-\beta+\varepsilon^2+\frac{1}{4}}+\varepsilon\right)+\mathrm{n}(\,\mathrm{n}+1)-\beta+2\varepsilon^2+2\varepsilon\sqrt{\gamma-\beta+\varepsilon^2+\frac{1}{4}}=0, \quad (28)$$

After some simplifications we have,

$$\left[4\left(A-B+\frac{1}{4}\right)-(2\,\mathrm{n}+1)^2\right]\varepsilon^2+2(2\mathrm{n}+1)[2\mathrm{A}-\mathrm{B}-\mathrm{n}^2-\mathrm{n}]\varepsilon+\left[(2\,\mathrm{n}+1)^2\left(\mathrm{A}-\mathrm{B}+\frac{1}{4}\right)-\left(n^2+n+\frac{1}{2}-B\right)^2\right]=0, \quad (29-1)$$

$$h_2\varepsilon^2+h_1\varepsilon+h_0=0. \quad (29-2)$$

By solving this equation and obtaining the $\mathcal{E}$ we will wined the energies E as,

$$\mathrm{E_{nlj}}=(-(\hbar\hat{}2\,\delta\hat{}2)/2\mu)(\varepsilon^2+\frac{2\mu V_0^{'}}{(\hbar^2\delta^2)(0.0067413175)}+\frac{\mu \mathrm{V}^{'(0)}_{\mathrm{LS}}\mathrm{r}_0^2\left(\mathrm{j}(\mathrm{j}+1)-\mathrm{l}(\mathrm{l}+1)-\frac{3}{4}\right)}{\hbar^2}\times(0.4341808999\times10^{-4}). \quad (30)$$

Ground state energy of the ^{17}F can be obtained by using of $j=\frac{5}{2}$, n = 0 , l =2 and the first excited states can be calculated by using of the $j=\frac{1}{2}$, n = 1 , l = 0 . Now, the wave-functions can be obtained through,

$$\psi(\mathrm{s})=\mathrm{y}(\mathrm{s})\phi(\mathrm{s}), \quad (31-1)$$

$$\rho(\mathrm{s})=\mathrm{s}^{1+2\varepsilon}(1-\mathrm{s})^{2\sqrt{\gamma-\beta+\varepsilon^2+\frac{1}{4}}}, \quad (31-2)$$

$$\phi(\mathrm{s})=\mathrm{s}^{\varepsilon}(1-\mathrm{s})^{\left(\sqrt{\gamma-\beta+\varepsilon^2+\frac{1}{4}}-\frac{1}{2}\right)}, \quad (31-3)$$

$$\mathrm{y_n}(\mathrm{s})=\mathrm{P_n}^{\left(1+2\varepsilon,2\sqrt{\gamma-\beta+\varepsilon^2+\frac{1}{4}}\right)}(1-2s), \quad (31-4)$$

$$\psi_{\mathrm{nl}}(\mathrm{s})=\mathrm{N_{nl}}\mathrm{s}^{\varepsilon}(1-\mathrm{s})^{\sqrt{\gamma-\beta+\varepsilon^2+\frac{1}{4}}+\frac{1}{2}}\times\mathrm{P_n}^{\left(1+2\varepsilon,2\sqrt{\gamma-\beta+\varepsilon^2+\frac{1}{4}}\right)}(1-2s), \quad (31-5)$$

where $P_n^{(\mu,\nu)}(x),\mu>-1,\nu>-1,x\in[-1,1]$ are Jacobi polynomials. Ground state and first excited state wave functions are presented in the figures (4) and (5) respectively. As we can see in the figures (4-5), good agreement exists.

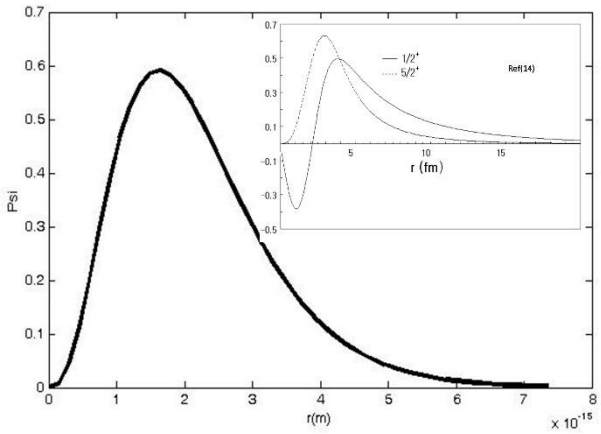

Fig. 4 – Normalized 5/2$^+$state wave function which we have calculated compared with ref [14] (inset panel) as a function of the radius r (fm)

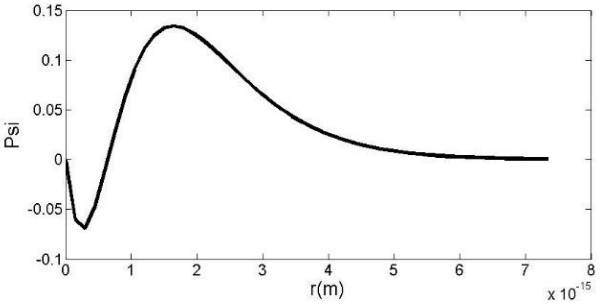

Fig. 5 – First excited state wave function by using of J=1/2$^+$. compare with ref [14] (inset panel of the figure 4)

Conclusions

In this study, the non-relativistic radial Schrödinger equation solved for Wood-Saxon potential together with coulomb potential (here for r>R_c; R_c= spherical nucleus radius), spin-orbit interaction and centrifugal term by a combination of the Nikiforov-Uvarov and numerical fitting methods. The energy eigen-functions and eigen-values of this model system obtained by NU method. For this purpose, by using approximate expansion of $1/r^2$, as well was using equivalent second order algebraic equation in the NU method (a big difficulty in this method), the Schrödinger equation has been transformed to an analytically solvable differential equation. However, in a case study which one is not able to obtain an appropriate equivalent second order algebraic equation in the NU method, this method will not be applicable to that problem. By using this method, good agreement with previously published works values obtained.

References

1. C.A. Bertulani, P. Danielewicz, Nucl. Phys. A **717**, 199 (2003)
2. C.A. Bertulani, Comp. Phys. Commun. **156**, 123 (2003)
3. M.R. Pahlavani, S.A. Alavi, Commun. Theor. Phys. **58**, 739 (2012)
4. A. A. Rajabi, M. Hamzavi, J. Theor. Appl. Phys. **7**, 17 (2013)
5. H. Hassanabadi, S. Zarrinkamar, A. A. Rajabi, Commun. Theor. Phys. **55**, 541 (2011)
6. M. Hamzavi, H. Hassanabadi, A. A. Rajabi, Int. J. Mod. Phys. E **19**, 2189 (2010)
7. R. Oudi, S. Hassanabadi, A.A. Rajabi, H. Hasanabadi, Commun. Theor. Phys. **57** , 15 (2012)
8. S. Zarrinkamar, A. A. Rajabi, B. H. Yazarloo, H. Hassanabadi , Chinese Physics C **37** (2013)
9. H. Hassanabadi, S. Zarrinkamar, H. Hamzavi, A. A. Rajabi, Arab J. Sci. Eng. **37**, 209 (2012)
10. A. F. Nikiforov, V.B. Uvarov, *Special Functions of Mathematical Physics* (Berlin: Birkhausr 1988)
11. S. M. Ikhdair, Int. J. Mod. Phys. C **20**, 25 (2009)
12. C. Tezcan, R. Sever, Int. J. Theor. Phys. **48**, 337 (2009)
13. Z. B. Wang, M. C. Zhang, Acta Phys. Sin. **56** (2007)
14. K. H. Kim, J. Korean, Phys. Society **43**, 691 (2003)

TTMP vol 1(1), 2024
doi: 10.30511/TTMP.2024.709743

Transactions in Theoretical and Mathematical Physics

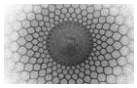

An impressive method for adjoint of linear and nonlinear operators

Mehdi Jafari Matehkolaee[a,1], Alameh Hajimohammdi-Fariman[b,2]

[1] Department of Physics, Amirkabir University of Technology (Tehran Polytechnic) P.O. Box:15875-4413, Tehran, Iran
[2] Department of Physics, Faculty of Physics & Chemistry, Alzahra University, Tehran, Iran

Received: 08 July 2023/ Accepted: 02 January 2024/ Published: 05 Feruary 2024

Abstract In this paper, we have obtained the adjoint of an arbitrary operator (linear and nonlinear) in Hilbert space by introducing an n-dimensional Riemannian manifold. This general formalism covers every linear operator (non-differential) in Hilbert space. In fact, our approach shows that instead of directly using an operator's adjoint definition, it can be obtained directly by relying on a suitable generalized space according to the action of the operator in question. In the case of nonlinear operators, we must change the definition of the linear operator adjoint. However, here, we have obtained an adjoint of these operators concerning the definition of the derivative of the operator. We have shown one of the straight applications of "Frechet derivative" in the algebra of the operators.

1 Introduction

This paper consists of two main parts. In the first part, we look for a general relationship for the adjoint of the linear operators. We intend to achieve a universal formula for the adjoint of the linear operators with a generalized space, such as the Riemannian manifold. Although the self-adjoint extensions of differential operators on the Riemannian manifold have been studied [1], we focus on non - differential operators. Recently, it has been reported that linear operators are unitary in curved space [2].

In the second part, we seek a special approach for the nonlinear operators.

Consider a linear operator O such that [3]

$$Of(x) = f(3x^2 + 1). \tag{1}$$

Even though we can calculate the adjoint of the operator O, we show in the next section that it is possible to do it directly by introducing the generalized space. Now, we define the linear operator $\Im_\varepsilon$ by

$$\Im_\varepsilon \mathrm{f(x)} = \mathrm{f}\big(\mathrm{x} + \varepsilon \mathrm{h(x)}\big), \tag{2}$$

where ε is an infinitesimal quantity. Obviously, considering $h(x) = 1$, the operator $\Im_\varepsilon$ is the translation operator in standard quantum mechanics [4]. But, in general, the arbitrary function $h(x) = 1$ could be the space metric, such that the operator $\Im_\varepsilon$ will be the translation operator in generalized space. In section II, we introduce a general approach to define the adjoint of these operators.

Most of the operators we deal with in quantum mechanics are linear. By definition, every linear operator must have the following two conditions [5]:

$$A[f(x) + g(x)] = A[f(x)] + A[g(x)], \tag{3}$$

$$A\big(af(x)\big) = aA\big(f(x)\big), \tag{4}$$

where a is a complex constant.

There are two different fundamental classes of non-linear operators: One is homogeneous non-linear operators, which do not satisfy the condition of equation (4), and the second one is nonhomogeneous nonlinear operators, which do not satisfy the condition of equation (3), [6]. As an example, for a homogeneous nonlinear operator, we can write

$$Af = |f| \int_0^{2\pi} e^{ia} B e^{-ia} \frac{f}{|f|} da, \tag{5}$$

where the domain of A is the same as the domain of B.

The operator A is not differentiable, so as we will see further, the adjoint of this operator cannot be defined. In fact, the point is that any differential operator that has the property of (4) is a linear operator. The argument is very simple.

[a] m.matehkolaee@aut.ac.ir

In the mathematical literature, the anti-linear or conjugate linear operator is a renowned example that does not satisfy the equation (4). This operator is reminiscent of the time reversal operator in quantum mechanics. It is well known that Dirac's bra-ket notation is not suitable for these operators [4]. A report examines this problem with a special approach [7].

Now consider a non-linear operator B which can be defined by

$$B[f(x)] = [f(x)]^2. \tag{6}$$

In section III, we discuss the general approach for the adjoint of the operator B.

2 Adjoint of linear operator

Consider the Riemannian manifold M with an atlas consisting of only one chart. This manifold is such that a global one-to-one correspondence exists between the points of M and $\mathbb{R}^n$.

So, the inner product of two arbitrary functions ψ and ϕ are defined through.

$$\langle\varphi|\psi\rangle = \int \zeta(x)\overline{\phi(x)}\psi(x), \tag{7}$$

where ζ is the invariant volume element $\zeta(x) = g(x)d^n x$, and g is the square root of the absolute value of the determinant of the metric matrix. We define an arbitrary operator O by

$$\langle x|O|\psi\rangle = \psi[h(x)], \tag{8}$$

so that

$$\langle\phi|O|\psi\rangle = \int \zeta(x)\bar{\phi}(x)\,\psi[h(x)], \tag{9}$$

where $h(x)$ is smooth, invertible, and differentiable function. Now we define z through $z = h(x)$ and using

$$\zeta\left[h^{-1}(z)\right] = \left[\frac{\left(h^{-1}\right)^* g}{g}\right](z)\zeta(z), \tag{10}$$

where h^* is the pullback of h[1], one arrives at

$$\langle\phi|O|\psi\rangle = \int \zeta(z)\left[\frac{\left(h^{-1}\right)^* g}{g}\right](z)\bar{\phi}[h^{-1}(z)]\,\psi[z], \tag{11}$$

The equation (11) shows that

$$\langle x|O^\dagger|\phi\rangle = \left[\frac{\left(h^{-1}\right)^* g}{g}\right](x)\bar{\phi}\left[h^{-1}(x)\right]. \tag{12}$$

This is correct if h is one-to-one, otherwise, there would be several inverses for h.

Denoting these by ${h_i}^{-1}$, hence we can write:

$$\langle x|O^\dagger|\phi\rangle = \sum_i \left[\frac{\left({h_i}^{-1}\right)^* g}{g}\right](x)\,\phi\left[{h_i}^{-1}(x)\right]. \tag{13}$$

Equation (13) can calculate the adjoint of any arbitrary linear operator (non-differential) with any representation or definition. For two simple examples, see Appendix A.

Now, we can compute operators (1) and (2) adjoints. For the first case, we have

$$h(x) = 3x^2 + 1, h^{-1}(z) = \pm\sqrt{\frac{z-1}{3}}, \left|\frac{d\left[h^{-1}(z)\right]}{dz}\right| = \frac{1}{6\sqrt{\frac{z-1}{3}}}, \tag{14}$$

So, we can write

$$\langle z|O^\dagger|\phi\rangle = \frac{1}{6\sqrt{\frac{z-1}{3}}}\left[\phi\left(\sqrt{\frac{z-1}{3}}\right) + \phi\left(-\sqrt{\frac{z-1}{3}}\right)\right]. \tag{15}$$

For the operator (2), at first, we consider an infinitesimal diffeomorphism f_ε, with

$$f_\varepsilon = x + \varepsilon h(x). \tag{16}$$

Note that, in this equation x and f are members of the manifold M. Their coordinates are, of course, scalars, as they are the components of the $h(x)$, which is itself a vector.

[1] According to the definition, the pullback of the function h is equal to:

$$(h^* f)_{\mu\nu}(x) = \{f_{\alpha\beta}[h(x)]\}\frac{\partial h^\alpha}{\partial x^\mu}\frac{\partial h^\beta}{\partial x^\nu}$$

The definition of pullback f gives the following equation:

$$(f^*g)_{\mu\nu} = g_{\mu\nu} + \varepsilon\left[\left(\nabla_\mu h\right)_\nu + (\nabla_\nu h)_\mu\right], \tag{17}$$

where ∇ is the covariant derivative corresponding to the Levi-Civita connection in relation to the metric g. So, by using (17) we can obtain immediately

$$f^*g = [1 + 2\varepsilon\nabla.h]g. \tag{18}$$

According to equation (2) and after some calculations we get the adjoint of the operator $\Im_\varepsilon$ in the form of

$$\Im_\varepsilon{}^\dagger f(x) = f\left[\left(x - \varepsilon h(x)\right)\left(1 - \varepsilon(\nabla.h)(x)\right)\right]. \tag{19}$$

3 Adjoint of nonlinear operator

For some reasons that will be revealed later we provide another definition in equations (3) and (4), for arbitrary linear operator A.

Definition: An arbitrary operator is linear if and only if its "Frechet derivative" is constant number or constant matrix. In another statement, operator A which acting on a function f is linear if its "Frechet derivative" does not depend on function f.

To clarify this definition, we consider two examples. In our opinion, probably, the equivalency of our definition with the common definition (equations (3) and (4)) is also true for other examples.

At first, consider linear operator A such that $Af(x) = f(g(x))$, where $f(x)$ and $g(x)$ are two arbitrary linear functions. So, we can write:

$$\begin{aligned} A[f(x) + h(x)] &= f(g(x)) + h(g(x)) \\ &= Af(x) + \int h(y)\delta(g(x) - y)d \end{aligned} \tag{20}$$

The derivative of A or $(DA)f(x)$ is given by

$$(DA)f(x) = \delta(g(x) - y). \tag{21}$$

Obviously, the equation of (21) shows that the derivative does not depend on the function f. It is simple to show that conditions (3) and (4) both, are consistent for this operator.

Now, consider another example:

$$Bf(x) = ln(f(x)). \tag{22}$$

We can write:

$$\begin{aligned} B[f(x) + h(x)] &= ln[f(x) + h(x)] \\ &= Bf(x) + \frac{h(x)}{f(x)}, \end{aligned} \tag{23}$$

where, we used the first order of h. Therefore, the derivative of B is given by

$$(DB)f(x) = \frac{1}{f(x)}. \tag{24}$$

The derivative of nonlinear operator B depends on function f. Again, it is simple to show that the conditions (3) and (4) aren't consistent for this operator.

As the complex conjugate operator is not differentiable and linear, in an orthodox manner, its adjoint is not defined. However, perhaps one could extend the definition of the adjoint operator to include this case as well. This definition is attributed to Wigner [8]. If we consider the usual definition for adjoint of an operator A as following

$$\langle u|A^\dagger v\rangle = \langle Au|v\rangle, \tag{25}$$

So for the anti-linear operators we should change the definition (25) to following form:

$$\langle u|A^\dagger v\rangle = \langle v|Au\rangle. \tag{26}$$

There are some references concerning nonlinear operator algebra [9, 10], with no specific suggestion to define the adjoint of nonlinear operators. In one reference, [11], for the special class of nonlinear operators in Banach space, which most of its operators are similar to linear operators, the adjoint of these operators is introduced on the basis of their derivatives.

At first, we notice that for the nonlinear operator B, whatever $B^\dagger$ would be, the statement $\langle u, B^\dagger v\rangle$ should be anti-linear in terms of u. So we need to construct some function like $\Re$ of u, v and B in such a way that by using the inner product, we get, namely

$$\langle u, B^\dagger v\rangle = \Re(u, v, B). \tag{27}$$

But if the definition somehow resembles the definition of the adjoint operator, we expect that some operation like the action of B on u occurs in $\Re$. The problem is that if the

action of B on u is nonlinear, then it does n't seem to be a natural way to construct something anti-linear in terms of u, say from (Bu) and the inner product. The reason that one could construct such a thing for linear or anti-linear B's, is that $\langle Bu, . \rangle$ is anti-linear in terms of u if B is linear, and if B is anti-linear, $\langle . , Bu \rangle$ would be anti-linear in u. So, the problem is to construct something quasilinear (linear or anti-linear) in u, from the action of something related to B on u.

One way to do so, is to use the derivative of B instead of B itself. According to our definition in section I, if B is linear, then its derivative is a constant matrix, which its action on a vector u is the same as $B(u)$, namely,

$$(DB)u = B(u). \tag{28}$$

For the general case where B is not linear, of course above relation does not hold. Then in the general case of nonlinear operator B, let's define $B^\dagger$ as $(DB)^\dagger$, that is

$$\langle u, B^\dagger v \rangle = \langle (DB)u, v \rangle. \tag{29}$$

But then, the problem is that (DB) is no longer a constant, if B is nonlinear operator. So, the correct form of the above relation should be

$$\langle u, [B^\dagger(f)]v \rangle = \langle [(DB)(f)]u, v \rangle, \tag{30}$$

where f is some point.

Now we come back to the equation (5), then

$$\begin{aligned}[B(f+\delta f)](x) &= [(f+\delta f)(x)]^2 \\ &= [f(x)]^2 + 2[f(x)][(\delta f)(x)] + \dots \\ &= [f(x)]^2 + \int dy \{2[f(x)]\delta(x-y)\} \\ &\qquad \times [(\delta f)(y)] + \dots, \end{aligned} \tag{31}$$

which means that

$$[(DB)(f)](x,y) = 2[f(x)]\delta(x-y). \tag{32}$$

The left-hand side is the matrix element of $[(DB)(f)]$. So,

$$\begin{aligned}&\{[(DB)(f)]u\}(x) \\ &\quad = \int dy \{[(DB)(f)](x,y)\}u(y) \\ &\quad = 2f(x)u(x). \end{aligned} \tag{33}$$

Then ,

$$\begin{aligned}\langle [(DB)(f)]u, v \rangle &= \int dx \overline{[2f(x)u(x)]}\, v(x) \\ &= \int dx \overline{[u(x)]}\, \overline{[2f(x)]} v(x). \end{aligned} \tag{34}$$

Therefore,

$$\{[B^\dagger(f)v]\}(x) = \overline{[2f(x)]}v(x), \tag{35}$$

or

$$[B^\dagger(f)](x,y) = \overline{[2f(x)]}\delta(x-y). \tag{36}$$

4 Conclusion

In this paper we have searched two original questions in two parts. 1) Is there a universal formula for the adjoint of the linear operator? 2) Is there a definition for the adjoint of the nonlinear operators? Regarding the first question, one can generalize the metric space and perform the adjoint computation on a Riemannian manifold to reach a universal formula. The equation (13) could be a universal formula for the adjoint of the linear operators. Regarding the second question, we have argued and indicated by using the definition of the derivative of the operator, we can obtain an adjoint of the nonlinear operator. Our method in this paper is suitable for nonlinear operators that are differentiable. It seems to nonlinear operators that are not differentiable do not exist in a "natural way" to define adjoint[2]. Our meaning of the "natural way" is preserving some of the properties of the standard definition of the adjoint. For instance, in the new definition, keeping the inner product's absolute value is necessary. A central concept in the linear operator's theory is the concept of the inner product. That is why we have used the operator's derivative to define the adjoint of nonlinear operators.

Acknowledgement I thank Professor Mohammad Reza Sarkardei for interesting discussions and comments, and Professor Mohammad Khorrami to critical reading.

[2] For example, consider an operator such as A which $A\psi(x) = |\psi(x)|^2$ which is not differentiable. One can write:
$|\psi(x) + h(x)|^2 = |\psi(x)|^2 + \psi(x)h^*(x) + \psi^*(x)h(x) + O(h)$
but the sum of the second and third terms (the pseudo-linear part) is neither linear nor anti-linear. Therefore, we don't know yet a "natural way" to define the adjoint of this operator.

Appendix A:

Here, we consider two examples with respect to the equation (13).

Example 1:

Consider $h(x)=\frac{1}{x}$ and $h^{-1}(z)=\frac{1}{z}$ so we can write $\left|\frac{d[h^{-1}(z)]}{dz}\right|=\frac{1}{z^2}$, therefore we get $\langle z|O^{\dagger}|\phi\rangle=\frac{1}{z^2}\phi(\frac{1}{z})$.

Example 2:

Suppose $h(x)=-x^2$ and ${h_{\pm}}^{-1}(z)=\pm\sqrt{-z}$ then we can write $\left|\frac{d[{h_{\mp}}^{-1}(z)]}{dz}\right|=\frac{1}{2\sqrt{-z}}$ therefore we obtain

$$\langle z|O^{\dagger}|\phi\rangle=\frac{1}{2\sqrt{-z}}\left[\phi(\sqrt{-z})+\phi(-\sqrt{-z})\right]$$

References

1. S. O. Milatovic, F. Truc, Ann.Glob.Anal.Geom **49** (2016)
2. M. Jafari Matehkolaee, Chinese Phys. B **30** (2021).
3. S. Gasiorowicz, *Quantum Physics* (John Wiley & Sons, 2003)
4. J.J. Sakurai, *Modern Quantum Mechanics*, (edited by San Fu Tuan Benjamin, Cumminges, Menlo Park, Ca. 1985)
5. Weidmann,J, *Linear operators in Hilbert Spaces* (Springer-Verlag, New York, 1980)
6. S. Bugajski, Int.J.Theor.Phys. **30**, 7 (1991)
7. A.Royer, Am. J. Phys. **62**, 8 (1994)
8. A. Uhlmann, Sci. China: Phys. Mech. Astron. **59**, 3 (2016)
9. C. Schwartz I, J. Math. Phys. **38**, 7 (1997)
10. C. Schwartz II, J. Math. Phys. **38**, 7 (1997)
11. V. Buryskova, The Rocky M. J. of Math. **28**, 1 (1998)